2015

3-D Numerical Simulation of Carbon Dioxide Injection into the South Georgia Rift Basin for Geologic Storage

Daniel Eric Taylor Brantley
University of South Carolina - Columbia

3-D Numerical Simulation of Carbon Dioxide Injection into the South Georgia Rift Basin for Geologic Storage

by

Daniel Eric Taylor Brantley

Bachelor of Science
Presbyterian College, 1997

Master of Earth and Environmental Resources Management
University of South Carolina, 2006

Master of Science
University of South Carolina, 2009

Submitted in Partial Fulfillment of the Requirements

For the Degree of Doctor of Philosophy in

Geological Sciences

College of Arts and Sciences

University of South Carolina

2015

Accepted by:

Camelia Knapp, Major Professor

John Shafer, Committee Member

Venkat Lakshmi, Committee Member

James Kellogg, Committee Member

Lacy Ford, Vice Provost and Dean of Graduate Studies

Dedication

I dedicate this work to my wife Becky. Without her unwavering love and support and unyielding patience and understanding this work would have never been completed. I would also like to dedicate this work to my two beautiful children, Joe and Day. Both of you inspire me more than you'll ever know. I also dedicate this to my parents, who instilled an unquenchable curiosity through exposure to the beauty and wonders of nature and the travel to experience that beauty and wonder first hand. My upbringing opened the doors of the imagination and for that, among many other things, I am forever grateful.

Acknowledgements

This material is based upon work supported by the U.S. Department of Energy (DOE) National Energy and Technology Laboratory (NETL) under Grant Number DE-FE0001965. This project is managed by the South Carolina Research Foundation and funded by DOE/NETL and cost sharing partners. I would also like to thank my dissertation committee, Dr. Camelia Knapp, Dr. John Shafer, Dr. Venkat Lakshmi and Dr. Jim Kellogg. Their guidance and encouragement was a critical and necessary component of this paper being completed. I would also like to thank the research faculty at the Earth Sciences and Resources Institute - University of South Carolina, specifically Mike Waddell and Adrian Addison for all of their contributions and guidance. I would also like to acknowledge and thank Schlumberger™ and the Computer Modeling Group™. This work could not have taken place without their software contributions at or near no cost.

Disclaimer

This report was prepared as an account of work sponsored by an agency of the United States Government. Neither the United States Government nor any agency thereof, nor any of their employees, makes any warranty, express or implied, or assumes any legal liability or responsibility for the accuracy, completeness, or usefulness of any information, apparatus, product, or process disclosed, or represents that its use would not infringe privately owned rights.

Reference herein to any specific commercial product, process, or service by trade name, trademark, manufacturer, or otherwise does not necessarily constitute or imply its endorsement, recommendation, or favoring by the United States Government or any agency thereof. The views and opinions of authors expressed herein do not necessarily state or reflect those of the United States Government or any agency thereof.

The South Carolina Research Foundation (SCRF) makes every effort to collect, provide, and maintain accurate and complete information. However, data acquisition and research are ongoing activities of SCRF, and interpretations may be revised as new data are acquired. Therefore, all information made available to the public by SCRF should be viewed in that context. Neither the SCRF nor any employee thereof makes any warranty, expressed or implied, or assumes any legal responsibility for the accuracy, completeness, or usefulness of any information,

apparatus, product, or process disclosed in this report. Conclusions drawn or actions taken on the basis of these data and information are the sole responsibility of the user.

Abstract

This study numerically simulated the injection of supercritical phase CO_2 into the South Georgia Rift (SGR) basin to evaluate the feasibility and efficacy of long term geologic storage. The injection simulation modeling was divided into two phases. During phase one of the modeling, very little geologic and reservoir dynamics data was known about the SGR basin. Due to lack of basin data, an equilibrium model was used to estimate the initial hydrostatic pressure, temperature and salinity gradients that represent our study area. For the equilibrium model, the USGS SEAWAT program was used and for the CO_2 injection simulation, TOUGH2-ECO2N was used. A stochastic approach was used to populate the permeability in the injection horizon within the model domain. The statistical method to address permeability uncertainty and heterogeneity was Sequential Gaussian Simulation. The target injection depths are well below the 1 km depth required to maintain CO_2 as a supercritical fluid. This study simulated 30 million tons of CO_2 injected at a rate of 1 million tons per year for 30 years. This is USDOE's stated minimum capacity requirement for a viable CO_2 storage reservoir. In addition to this requirement, a 970 year shut-in time (no injection) was also simulated to better determine the long term fate and migration of the injected CO_2 and to ensure that the SGR basin could effectively contain 30 million tonnes of CO_2. The preliminary modeling of CO_2 injection indicated that the SGR basin is suitable for geologic storage of this DOE stated minimum capacity.

During phase two, newly acquired seismic and well data were used to build a 3-D geologic model that included structure for the injection simulation model. Phase two of the injection simulation modeling looks at the effects of faulting on the numerical simulation of CO_2 injection into the South Georgia Rift basin. For this study, two software packages were employed to build the injection simulation model. Petrel™ was used to construct geo-cellular grid based on the 3-D geologic model. CO_2 injection simulation was achieved using the compositional reservoir simulator CMG-GEM. The total simulation time was 100 years during which a total of 30 million tonnes of CO_2 was injected at a rate of 1 million tonnes per year for 30 years followed by a 70 year shut-in period. Multiple experiments were run to find the effects of fault permeability on the resultant fate of the injected CO_2. Fault permeabilities were: 0 mD representing a sealing fault, 1 mD representing a low permeability fault, and 100 mD representing a conduit fault. The results from this research illustrate that with a permeability of 1 mD, significant leakage of CO_2 occurs up the faults. This is evidence that fault analysis is a critical factor in injection simulation modeling and ultimately in determining the efficacy of long term geologic storage of CO_2 and that even low permeability faults make the geology potentially unsuitable.

Conclusion of this research are: 1) the SGR basin is composed of numerous sub-basins, 2) this study only looked at portions of one sub-basin, 3) in SC, 30 million tonnes of CO_2 can be injected into the diabase units if the fracture network is continuous through the units, 4) due to the severity of the faulting there is no way of assuring the injected CO_2 will not migrate upward into the overlying Coastal

Plain aquifers, and 5) the SGR basin covers area in three states and this project only studied two small areas so there is enormous potential for CO_2 sequestration in other portions the basin and further research needs to be done to find these areas.

Table of Contents

List of Tables

List of Figures

Chapter 1

Introduction and Motivation for this Research

1.1 Introduction

This research aligns with the newest carbon management legislation and initiatives on the basis of the assumption that increased carbon dioxide ($CO_{2)}$ levels are a major cause of climate change. Increasingly scientists are connecting rising temperatures with increasing amounts of greenhouse gases in the atmosphere. These gases absorb part of the long-wave heat radiation emitted from the surface of the earth and can therefore cause atmospheric temperatures to increase (Houghton, 1997; Boden, 1994; Neftel, 1994; Keeling, 2004; Canadell, 2007; Solomon, 2009). Carbon dioxide is the most important because of the evidence that links increased atmospheric CO_2 concentrations with increased atmospheric temperature. In a global effort to mitigate the anthropogenic release of CO_2 into the atmosphere, carbon capture, utilization and storage (CCUS) technology has become a major area of research in the climate change arena. (Goldberg et al., 2008; Zoback and Gorelick, 2012; Pires et al., 2011; Brantley et al. 2015; Nasvi et al., 2013; Leung et al., 2014; Cinar and Riaz, 2014; Riaz and Cinar, 2014; Park et al., 2006). In particular, deep saline formations provide a large storage area worldwide (Mohammed *et al*., 2012; Bachu, 2000; Behtham and Kirby, 2005; Ghomian *et al*., 2008; Micheal *et al*., 2010; Zhuo et al., 2007). Of all emissions

reduction mechanisms, including upgrading existing power plants for improved efficiency in power generation, building higher efficiency new plants, relying more on renewable energy and nuclear power, carbon capture and storage (CCS) is projected to provide the largest contribution to emissions reduction in the near/mid-term.

The U.S. Department of Energy National Technology and Energy Laboratory (U.S. DOE NETL) has acknowledged that the Mesozoic basins along the eastern seaboard of the United States contain sequences of sandstone layers bound by diabase and shale layers that may serve respectively as reservoir and seal layers ideal for CO_2 injection and long term storage. The South Georgia Rift (SGR) basin, one of the aforementioned Mesozoic basins, is classified by the U.S. DOE NETL as a "high potential" basin that represents a significant storage opportunity that could be commercially developed in the future (U.S. DOE-NETL, 2008).

This study investigates the feasibility of injection and long-term CO_2 storage in the northern portion of the SGR basin. The SGR basin lies near the southern end of the Eastern North American Rift System and is presupposed to be the southernmost and the largest of the eastern North American Triassic rift basins [(Figure 1.1) (Daniels and Zeitz, 1983; Klitgord *et al*., 1984; Olsen, 1997; Withjack *et al.,* 1998; Schlische, 2003)]. In sharp contrast to other basins being evaluated for carbon storage, the northern portion of the SGR basin has never been extensively studied and has only one boring (the Norris Lightsey # 1) that penetrates the depth of interest. The N.L. # 1 is a petroleum exploration well that

was drilled to a depth of 4,115 m and is the only well that goes through the 3000+ m of the Jurassic/Triassic J/Tr section of the basin (Shafer and Brantley, 2011). The Norris Lightsey #1 (N.L. #1) boring log indicates sequences of sandstone, diabase, and shale that could equate to a vertically stacked series of CO_2 reservoirs and seals, which would provide multiple reservoir CO_2 storage capability within the same injection well. The vertically stacked reservoir/seal combinations are ideal because they potentially reduce the CO_2 footprint for large volumes of CO_2 injection by using the same well to inject CO_2 into a series of vertically stacked reservoir horizons (Shafer and Brantley, 2011). With conservative porosity and permeability estimates, the U.S. DOE capacity equations (U.S. DOE, 2006) indicate the SGR basin has massive potential (> 100 million tonnes) for CO_2 storage. The large CO_2 storage volume estimates, combined with the vertically stacked storage potential and lack of deep wells that could serve as potential leakage pathways, make the SGR basin unique and potentially very attractive for long term CO_2 storage.

The southeastern U.S. contributes a large portion of our nation's total CO_2 (Figure 1.2). More than half of all (stationary and non-stationary) CO_2 emissions in South Carolina are from electric power plants and industrial manufacturing facilities. Permanently storing CO_2 in close proximity to the sources will provide economic efficiencies and reduce risks associated with transporting CO_2 long distances from source to sink. This research will ultimately aid in the determination of the extent to which the SGR is a suitable basin for long-term storage of supercritical CO_2.

The University of South Carolina has led a SGR basin characterization study to determine the feasibility of long-term geologic storage of CO2. The basin characterization study was divided into three stages. The first stage evaluated of all existing (legacy) data pertaining to the SGR basin using well logs and statistics (Brantley et al., 2015, Nelson and Kibler, 2003). During the second stage, approximately 386 kilometers (km) [~240 miles (mi)] of new seismic data were acquired and evaluated for optimum location of a deep characterization borehole. During the third and final stage a characterization borehole (i.e., Rizer # 1) was drilled. Petrophysical and geochemical testing within the borehole were performed and core and cuttings samples were examined for petrology.

The SGR basin is of particular importance for several reasons: 1) The large areal extent of the SGR basin (Figure 1.1) could prove to have large CO2 storage capacity; 2) The “high potential” basin classification that represents a significant storage opportunity in a region with adequate seals that could be commercially developed in the future; and 3) The proximity of the SGR basin to major sources of CO_2 in the southeastern United States. The SGR basin provides a unique opportunity for geologic carbon storage because the basin is not perforated with wells and boreholes, which could be potential leakage pathways that must be considered for long-term geologic storage of CO_2.

Due to the lack of information on the SGR basin at the onset of the CO_2 injection simulation modeling, this effort was divided into two phases. Phase One of CO_2 injection simulation into the SGR basin was a preliminary assessment using a simplified geocellular model and pre-specified basin parameters - porosity and

permeability (Brantley et al., 2015). Due to lack of basin data, an equilibrium model was used to estimate the initial hydrostatic pressure, temperature and salinity gradients that represent our study area. For the equilibrium model, the USGS SEAWAT program was used and for the CO_2 injection simulation, TOUGH2-ECO2N was used. A stochastic approach was used to populate the permeability in the injection horizon within the model domain. The target injection depths are well below the 1 km depth required to maintain CO_2 as a supercritical fluid. This study simulated 30 million tons of CO_2 injected at a rate of 1 million tons per year for 30 years. This is U.S. Department of Energy stated minimum capacity requirement for a viable CO_2 storage reservoir. In addition to this requirement, a 970 year shut-in time (no injection) was also simulated to better determine the long term fate and migration of the injected CO_2 and to ensure that the SGR basin could effectively contain 30 million tonnes of CO_2.

The focus of the second phase of the injection simulation is to use the model to study the impact of the geologic structure, particularly faults, on the fate of the buoyancy driven CO_2 plume. The SGR basin characterization study has revealed that the basin is highly fractured and faulted; therefore, the effect of the faulting on CO_2 migration must be considered when determining the efficacy of geologic storage of CO_2. The second phase of CO_2 injection simulation into the SGR basin used newly acquired data and a 3-dimensional (3-D) geologic model built in Schlumberger's Petrel™. Petrel™ is a state-of-the-art industry grade reservoir engineering software platform that enables collaboration of scientists and engineers to develop and contribute to a single dynamic earth model

(Schlumberger, 2014). The 3-D geologic model grid was then imported into CMG-GEM™ compositional reservoir simulator for CO_2 injection simulation. Total simulation time was 100 years during which a total of 30 million tonnes of CO_2 was injected at a rate of 1 million tonnes per year for 30 years followed by a 70 year shut-in period. Multiple experiments were run to find the effects of fault permeability on the resultant fate of the injected CO_2. The results illustrate that with a permeability of 1 mD, significant leakage of CO_2 occurs up the faults. This is evidence that fault analysis is a critical factor in injection simulation modeling and that even low permeability faults make the geology potentially unsuitable for long term geologic storage of CO_2.

1.2 Site Description

During Triassic and Early Jurassic time, a series of rift basins formed along a wide zone extending from the future Gulf of Mexico through Nova Scotia, Morocco, the Tethyan margin, Western Europe, and Greenland to form the Central Atlantic Margin (CAM). The Eastern North American Rift System (ENARS) portion of the CAM is comprised of a northeast trending series of Triassic-age rift basins that record the tectonic history just prior to the breakup of Pangea and the opening of the Atlantic (Olsen, 1997; Schlische *et al.*, 2003). These basins are filled by continent-derived fluvial and lacustrine redbeds, referred to as the Newark Supergroup, and Jurassic-age diabase and basalt of the Central Atlantic Magmatic Province (Olsen, 1997). As the SGR basin formed, it filled with sediment from the adjoining area and from rivers flowing along the axis of the rift. The basin is very deep in places, with sediments accumulating on the order of 5-6 kilometers (km)

[~3-4 miles (mi)] thick and comprised of mostly fine to coarse grained sandstone, mudstone and siltstone redbeds with intercalated layers of basalt and/or diabase. While the SGR basin was forming, there was also episodic but significant igneous activity. Mafic igneous rock intrusions known as dikes and sills entered the sedimentary layers, and lava flowed on the top of the sedimentary material in some locales. Unlike many other Mesozoic basins that crop out along the eastern edge of North America, the SGR basin is completely buried, making characterization much more difficult.

The breakup of Pangaea, including the formation of the Mesozoic basins of eastern North America, has been extensively researched with the exception of the SGR basin. Due to (1) the depth of the SGR basin combined with (2) the lack of interest from the exploration industry, only sparse drilling and geophysical research has been conducted. Previous to this study, the structure of the SGR basin had only been speculated from scattered drilling and potential field (gravity and magnetics) interpretation, leaving the internal boundary and the deep structure unknown (McBride, 1991). Chowns and Williams (1983) completed a comprehensive study of deep wells in Georgia, Florida, and Alabama to assess the extent of the SGR basin and relied on interpretations of gravity and magnetic surveys for determining the boundaries where little to no well control was available (Hefner, 2013). There are less than ten boreholes that were drilled into the Triassic-age sediments and only one wildcat well, the N.L. #1 drilled in the 1984, that penetrated a significant portion [~4,000 meters (m) (~13,123 feet)] of the SGR basin in our South Carolina study area. Lack of data makes the SGR basin unique

in that unlike other U.S. DOE sponsored carbon capture and storage projects, the basin has yet to be studied. Further, there is so little currently known about the geology of the SGR basin that the formations have yet to be named. Nevertheless, the Carbon Sequestration Atlas of the United States and Canada (U.S. DOE NETL, 2008) identifies the Triassic basin in southern South Carolina as a saline formation suitable for CO_2 storage.

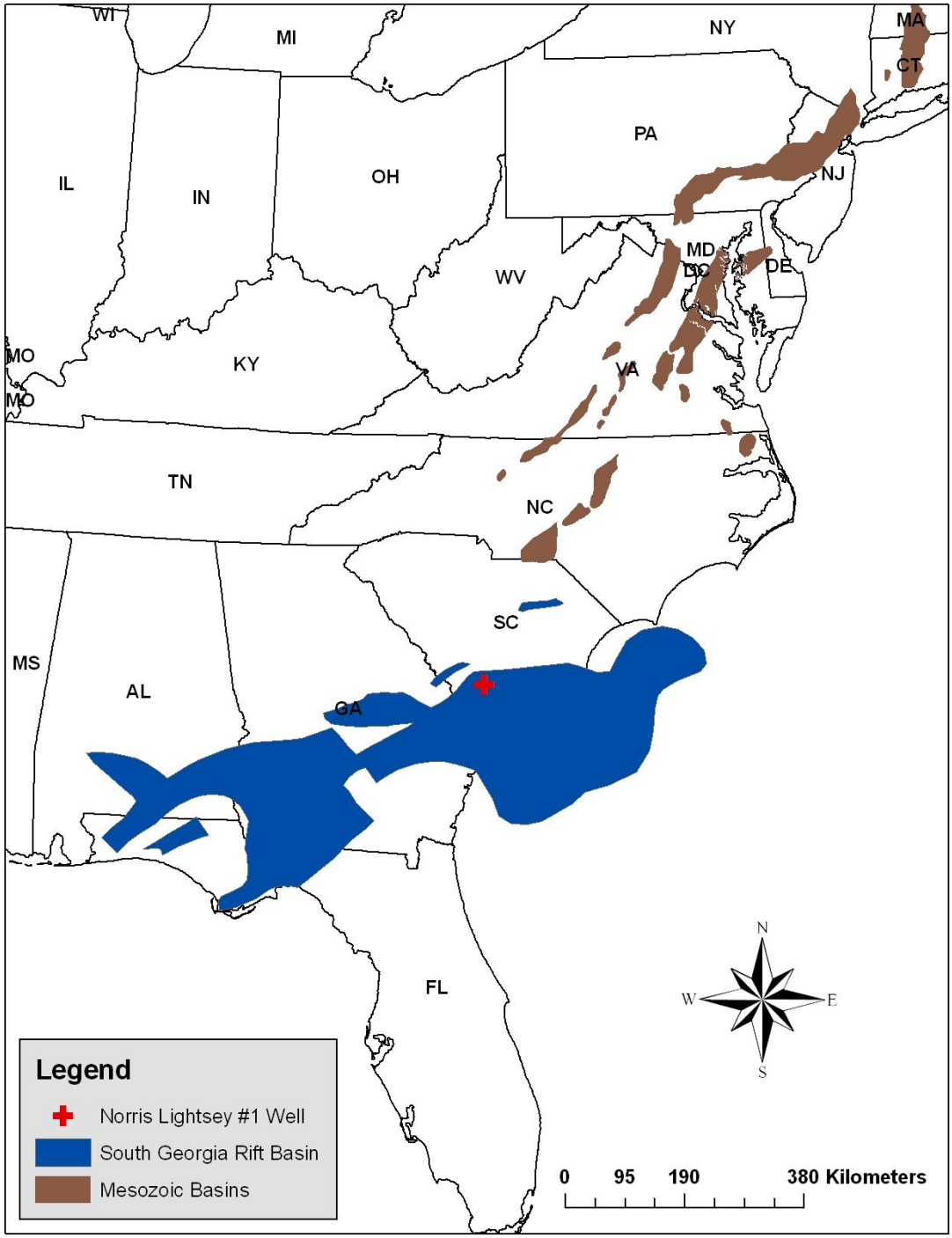

Figure 1.1: CO_2 Sources in South Carolina and Georgia proximal to the study area.

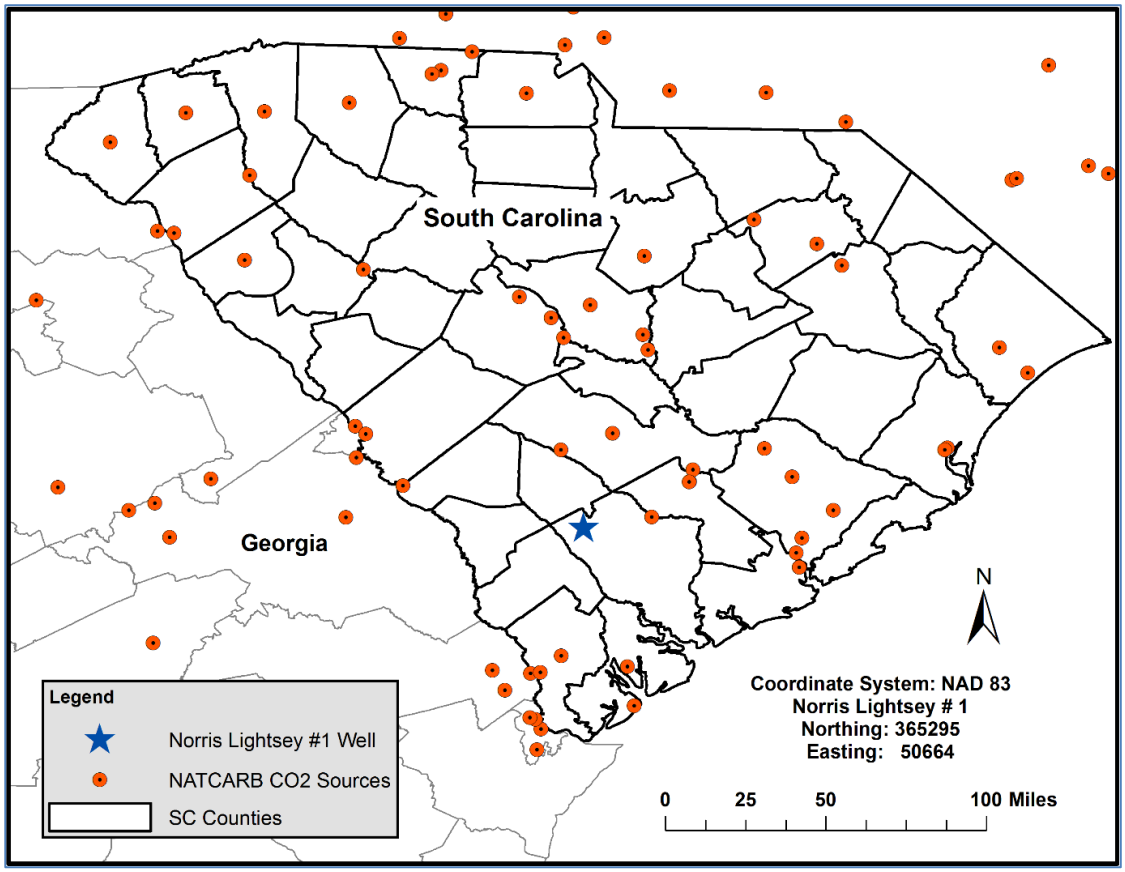

Figure 1.2: Eastern North American Rift System Mesozoic Basins and the South Georgia Rift Basin.

Chapter 2:

CO_2 Injection Simulation into the South Georgia Rift Basin for Geologic Storage: A Preliminary Assessment

2.1 Objectives

The objectives of phase one of the injection simulation modeling were to simulate CO_2 injection, plume migration, and long-term fate of supercritical CO_2 in the SGR basin. The injection simulation will be assist in determining the suitability of the SGR basin for long-term geologic carbon sequestration. For this study, long-term is defined as 1000 years and over pressured is defined as pressure that would cause upward leakage of CO_2 through the igneous seal or pressure that exceeds lithostatic pressure, which is ~65 megapascals (MPa) [9,427 pound force per square inch (psi)].

Criteria for suitability are:

1. Meet U.S. DOE's minimum required injection rate and capacity of 1 million tonnes annually over 30 years.
2. The process of CO_2 injection does not over-pressurize the system.
3. The CO_2 does not migrate unexpectedly, particularly through the seal.

The CO_2 injection simulation will:

1. Forecast the reservoir conditions and the system's response to the stress of CO_2 injection.
2. Forecast the fate and transport of the CO_2 during injection as well as a prescribed time post-injection.
3. Aid as a decision support tool in determining if the SGR basin is suitable for long-term geologic storage of supercritical CO_2.
4. Aid as a decision support tool in the design of CO_2 injection field studies and full scale implementation.

2.2 CO_2 Injection Simulation

CO_2 injection feasibility and CO_2 migration within (and out of) the target storage formations are key concerns of deep geologic sequestration. Safe and permanent underground storage of CO_2 must be certain before commercial development of a particular site can be undertaken. Numeric injection simulation models aid in addressing these concerns. The first step of the numeric modeling process is to create a Conceptual Site Model (CSM). A CSM is three-dimensional (3-D) geological model of the study site that is based on existing data and helps to better understand the physical conditions and behavior of the system being studied (Mercer and Faust, 1981). Using C-Tech Development Corporation's MVS software, a 3-D conceptual model was built to visualize the basic basin geology as indicated by the N.L. # 1 litho-stratigraphic log. MVS is state-of-the-art visualization software designed to aid engineers and environmental modelers in subsurface analysis, visualization, and animation (Copsey, 2014). For the MVS

conceptual model, we used a simplified lithology of three different materials: unconsolidated coastal plain, igneous rock, and sandstone. Figure 2.1 illustrates the CSM and displays basic basin stratigraphy as well the stacked storage concept of injecting into the multiple horizons. Armed with a better understanding of the subsurface conditions, the next step was to construct a numerical model of the study area.

Due to the deficiency of data in our study area, a two-pronged approach was taken to numerically simulate CO_2 injection and plume behavior in a target reservoir interval in the SGR basin's stacked reservoir stratigraphy. The SGR basin is a deep, variable-density groundwater flow, heat, and salinity transport system. However, hydrostatic pressure and brine concentration gradient are unknown. For this reason, the first step of the CO_2 injection simulation modeling was to establish pressure, temperature, and salinity regimes that are representative of the in-situ environment of the deep saline SGR basin using an equilibrium model. The results of the equilibrium model were then used as the initial conditions for the CO_2 injection simulation. Table 2.1 is a flowchart explaining the workflow for this two-pronged modeling approach to CO_2 injection simulation.

The initial conditions necessary for the injection simulation modeling using the TOUGH2 code require a hydrostatic pressure gradient, which is not known in the SGR basin. For this reason, we used USGS' SEAWAT to establish pressure, temperature, and salinity equilibrium conditions and thus, the initial hydrostatic pressure gradient. SEAWAT is an extension of the USGS-MODFLOW for numerical simulation of 3-D, variable density, transient groundwater flow

integrated with MT3DMS solute transport code. The advantages of using SEAWAT over traditional analytical methods are that it's readily available, easy to use, and considers density effects in the flow calculation. For the SEAWAT equilibrium model, a 100 x 100 x 100 grid was created that represents a 10 km (~6.2 mi) x 10 km (~6.2 mi) x 3 km (~1.9 mi) (x,y,z) spatial extent of the model domain. This grid size was selected to balance the size of the domain with the desired resolution. To the extent of what is known about the subsurface of the study area and in accordance with the conceptual site model, the layers are one of three materials: unconsolidated Coastal Plain sediment, Triassic lithified sediments, or J/T_r mafic material. The model domain vertical discretization is variable to coincide with the litho-stratigraphy of the N.L. # 1 well (Figure 2.2).

The thermal gradient was derived from the bottom-hole temperature of the N.L. #1 well log. The salinity gradient was presupposed from the Department of Energy's National Energy Technology Lab's identification of the SGR basin as being a hyper-saline system. Storativity and porosity parameters were derived from relevant literature and the N.L. # 1 well log (Nelson and Kibler, 2003; Ryan *et al.*, 2002). The elevation of the water table in the study area is approximately -10 m (~32.8 ft.), therefore an initial head of -10 m (32.8 ft.) was assigned to the entire domain. The surface layer of the domain was assigned -10 m (32.8 ft.) as a fixed boundary head, for every cell below a continuously saturated system was assumed. The equilibrium model was run to steady state with only fixed top (i.e., water table) boundary hydraulic heads.

The model output is a steady-state equilibrium volume that represents the hydrostatic pressure as a function of depth, temperature, and salinity in the SGR basin. Table 2.2 shows the hydrostatic pressure vs. depth considering temperature and salinity for every 10 horizons within the full vertical dimension of the domain. As expected, the pressure gradient increases with depth, as the salinity increases. As the basin becomes hyper-saline near its modeled base, the hydrostatic pressure non-linearly increases with depth. The results of the SEAWAT equilibrium model were then used as the initial conditions for the CO_2 injection simulation modeling.

TOUGH2-ECO2N, as implemented in PetraSim® is the software platform that was used for CO_2 injection simulation. ECO2N is the fluid property module for the TOUGH2 simulator that is designed for applications to geologic sequestration of CO_2 in saline formations. It addresses the thermodynamics and thermophysical properties of H_2O – NaCl – CO_2 mixtures, reproducing fluid properties largely within experimental error for the temperature, pressure, and salinity conditions of interest (Pruess, 2005; Pruess and Spycher, 2006). For this study, it was assumed that the CO_2 being injected is in supercritical phase. Due to the depth of the injection horizon, the pressure and temperature of the geologic strata far exceeds what is necessary to maintain this phase (i.e., T_{crit} = 31.04 ^oC (87.9 ^oF), P_{crit} = 7.382 MPa [(1,071 psi); (Vargaftik, 1975)]. For the TOUGH2 injection simulation model, a variable grid was created that represents a 10 km (~6.2 mi) x 15 km (~9.3 mi) x 3 km (~1.9 mi) (x,y,z) domain (Figure 2.3). Variable grids are used to allow incorporation of more spatial information in a computationally efficient way. This

approach creates a hierarchal concept of space that creates a grid with much smaller cells (Voronoi cells) centered on and around the injection well, with the smallest cell being approximately the size of the injection well for a realistic injection representation. The variable grid is capable of simulating regional as well as local dynamics simultaneously (Vleit *et al*., 2009).

As with the SEAWAT model, the TOUGH2 model domain vertical discretization is variable to agree with the lithostratigraphy of the N.L. # 1 well and each cell was assigned a material and populated with that materials postulated hydrogeologic properties determined from N.L. # 1 geophysical log and relevant literature. The largest database of siliciclastic porosity and permeability data found was an assimilation done by the U.S. Geologic Survey (USGS) in Open-file Report 03-420. This report consist of over 70 datasets taken from published data and all measurements were taken from core samples. From this report, all of the data on Triassic-aged sediments were filtered out and the porosity and permeability data were plotted. Each dataset contained (1) a minimum of 20 porosity and permeability values, (2) a description of the depositional setting, (3) method of measurement, (4) referenceable source, and (5) the formation name, again, depth, and location of each sample taken (Nelson and Kibler, 2003). Figure 2.4 is a scatterplot of all datasets from the USGS that contain porosity and permeability data for cored samples of Mesozoic sandstone throughout the world. The porosity dataset is normally distributed and permeability dataset ranges over six orders of magnitude and log normally distributed. The dissolution of CO_2 in the formation water, also known as solubility trapping, is an important CO_2 migration and

trapping mechanism in the post-injection period of geologic storage in deep saline formations. Capillary pressure (P_c) and relative permeability are two major driving forces of fluid migration in CCUS; therefore, an accurate representation of the each is crucial for modeling solubility trapping, and hence long term CCUS (Boxiao *et al.*, 2012; Bachu and Bennion, 2008). To address capillary pressure and relative permeability, the van Genuchten Function (Pruess, 2005) and Corey's curves (Pruess, 2005) were used respectively in accordance with the ECO2N user manual's default values.

For both the equilibrium and the injection simulation, it was assumed that the permeability of the mostly unconsolidated material of the South Carolina coastal plain of (SGR basin overburden) was anisotropic and that the sandstone and mafic material within the SGR basin was isotropic. Table 2.3 is a summary of the parameters used for SGR basin CO_2 injection simulation.

Material property information (i.e., porosity and permeability) for CO_2 injection simulation in data-deficient geologic environments is sparse. Therefore, the material properties between and among data points must be determined through interpolation if the assumption of a homogeneous environment is unrealistic, which is usually the case. For this reason, stochastic simulation techniques have become the method of choice for generating numerical models that represent subsurface heterogeneities (Doyen, 2007). A commonly applied technique is Sequential Gaussian Simulation (SGS), which is a method for simulating spatially continuous properties (e.g., permeability) requiring knowledge of a variogram and histogram. In SGS, numerous equally probable and spatially

correlated realizations are created to incorporate uncertainty in the model parameter. Throughout the history of spatial stochastic modeling, Gaussian random fields are probably the oldest and the most commonly used models to represent spatial distributions of continuous variables (Damsleth, 1994). To demonstrate the effect of uncertainty in permeability heterogeneity in the injection reservoir on simulated CO_2 plume migration, a spatially correlated random field of permeabilities ranging from 10 milliDarcy (mD) to 100 mD was created using the Stanford Geostatistical Modeling Software (SGeMs) (Remy *et al.*, 2007) for SGS. The mean permeability of eight realizations was 23.4 mD, and the mean of the standard deviation of the eight realizations was 5.02 mD.

For this study, we used the sedimentary section between igneous seals E and F for the CO_2 injection simulation reservoir and the basalt horizon E as the top seal. The depth range of the target injection sedimentary section is between 2,476 m (8,123 ft.) – 2,588 m (8,491 ft.) below land surface, or well below the 1km (~0.62 mi) critical depth to maintain CO_2 as a supercritical fluid. Using the TOUGH2 preconditioned bi-conjugate gradient solver, multiple iterations of injection simulation were performed. The simulations began with a simple layer cake geologic representation of the basin and progressed into a more complex geology as confidence in the simulation approach was gained. For example, a 45º azimuth was applied to the permeability field to better represent the postulated SGR reservoir conditions. Also, to illustrate the significance of adding noncomplex, yet realistic geologic structure to the CO_2 injection simulation process, a 2% dip, trending in a southerly direction, was added to the entire model domain. This is the

approximate dip of the base of the Coastal Plain. For the CO_2 injection simulation an injection rate of 1 million tonnes per year for 30 years was established. In addition to this requirement, a 970 year shut-in time (no injection) was also simulated to better determine the long-term fate and migration of the injected CO_2 and to ensure that the SGR basin could effectively contain the 30 million tonnes of supercritical CO_2.

2.3 Results and Discussion

Many numerical experiments were conducted using the TOUGH2-ECO2N simulation code. Reservoir parameters were varied along with injection zone, injection time and shut-in time. Table 2.4 is a summary of the parameters that were adjusted for various simulation scenarios. The simulations were conducted to evaluate model robustness and the effects of different modeling scenarios and assumptions on the injection and resulting supercritical CO_2 plume dynamics. For example, experiments were run with reservoir porosity ranging from 1% to 25%. Due to uncertainty of the rock properties and hydrodynamics, an average of 6% porosity was used for the input of the modeling results discussed in this paper. This was an intentionally conservative approach as the USGS assimilated database suggest the average porosity for analog basin sandstone is ~ 15%. Throughout the preliminary injection simulation, many experiments were conducted using the range of input parameters discussed above, however, the results discussed in this paper are the results of the final and most progressed experiments of the preliminary modeling process.

Figure 2.5 shows the maximum pressure build-up at the injection wellhead as compared to the lithostatic pressure and demonstrates that the maximum injection pressure stays well below the injection zone lithostatic pressure, therefore insuring that the system does not become over-pressured due to CO_2 injection. Figure 2.6 shows the dissipation of the pressure back towards basin equilibrium during the subsequent 970 year shut-in period. Figure 2.6 suggests that the pressure recovery takes significantly more time than build-up due to injections. Note that the basalt seal horizon tightly holds the injection pressure and only during the shut-in period does it slightly increase in response to the pressure increase due to CO_2 injection. This slight increase in pressure in the basalt seal indicates that the simulation is working correctly and that the seal easily keeps the increased system pressure from propagating upwards. In other words, the seal adequately contains not only the supercritical CO_2, it also contains the pressure increase resulting from the injection. Figure 2.7 shows the effect of uncertainty in permeability (k) heterogeneity in the injection reservoir after a 1,000 year simulation. The image on the left assumes homogenous conditions with a constant k (10 mD), while the image on the right show the results of the same simulation with k ranging from 10 mD to 100 mD. In comparing the two Figure 2.7 images, the addition of a heterogeneous permeability distribution to the injection reservoir did not significantly change the radial extent of the injected CO_2, however a permeability modifier did provide a reasonable way to address in-situ permeability heterogeneity and therefore this approach should be used in all future CO_2 injection simulation of the SGR basin.

In contrast to the results illustrated in Figure 2.7 pertaining to heterogeneity, Figure 2.8 illustrates the importance of adding structural geology to the CO_2 injection simulation process. As in Figure 2.7, both Figure 2.8 images are the result of simulating the injection of CO_2 into the SGR reservoir at a rate of 1 million tonnes per year for 30 years with a 970 year shut-in. The left image in Figure 2.8 is the result of using the previous 10 mD to 100 mD heterogeneous permeability field for the injection reservoir. To illustrate the significance of adding simple, yet realistic, geologic structure to the CO_2 injection simulation process, a 2% dip was added to the entire model domain. As can be seen on the right of side of Figure 2.8, a 2% dip has a dramatic effect on the resultant morphology of the injected CO_2 plume. Being buoyant, the injected supercritical CO_2 rises until it hits the seal, and then slowly migrates up-dip along the bottom of the seal for the entire 1,000 year simulation. This simulation demonstrates that adding structural geology to the simulation can have a dramatic (and realistic) effect on the simulation outcome, resulting in a much larger areal footprint of the injected CO_2, particularly up-dip of the injection well. However, even with the geological structure added, the CO_2 still did not migrate more than 5 km (~3.2 mi) away from the injection well. Figures 2.7 and 2.8 are both from a top view looking straight down on the simulated injection site. The CO_2 plume seen in the both figures is in the injection reservoir, and none of the CO_2 penetrated the seal for the entire simulation period (Figure 2.8). Figure 2.9 is a slice plane of saturated CO_2 directly through the center of the injection well at the end of a 1,000 year simulation.

All CO_2 injection simulation experiments we conducted indicate that the SGR basin is suitable for long term CO_2 injection and storage. This conclusion was determined by meeting the three suitability criteria. Using the parameters discussed above the SGR basin could easily handle the U.S. DOE minimum requirement of 30 million tonnes of CO_2. The plume footprint is minimal even with conservative estimates for porosity (6%) and permeability (10 - 100 mD) (Figure 2.8). At the end of the 30 year injection, the areal extent of the CO_2 footprint was <20 square km (~7.7 square mi) and the maximum migration of CO_2 away from the injection well was < 5 km (~3.2 mi) (up-dip). Further, the pressure build-up at the well-head is much less than half of the calculated lithostatic pressure, which at the injection depth is approximately 65 MPa (9,427 psi) (Table 2.5). In the suitability criteria, over pressured is defined at (1) pressure that causes upward leakage of CO_2 through the caprock, and (2) injection pressure staying below the lithostatic pressure. When compared to numerical simulations of investigations from other saline basins, the plume size, pressures, and CO_2 saturation results of this SGR basin study are in range with their results (Zhuo *et al.*, 2007; Yamamoto *et al*., 2009; Bacon *et al*., 2009; Sasaki *et al*., 2008; Omambia and Li, 2010).

2.4 Tables and Figures

Table 2.1 Flow chart of the modeling steps taken in this study.

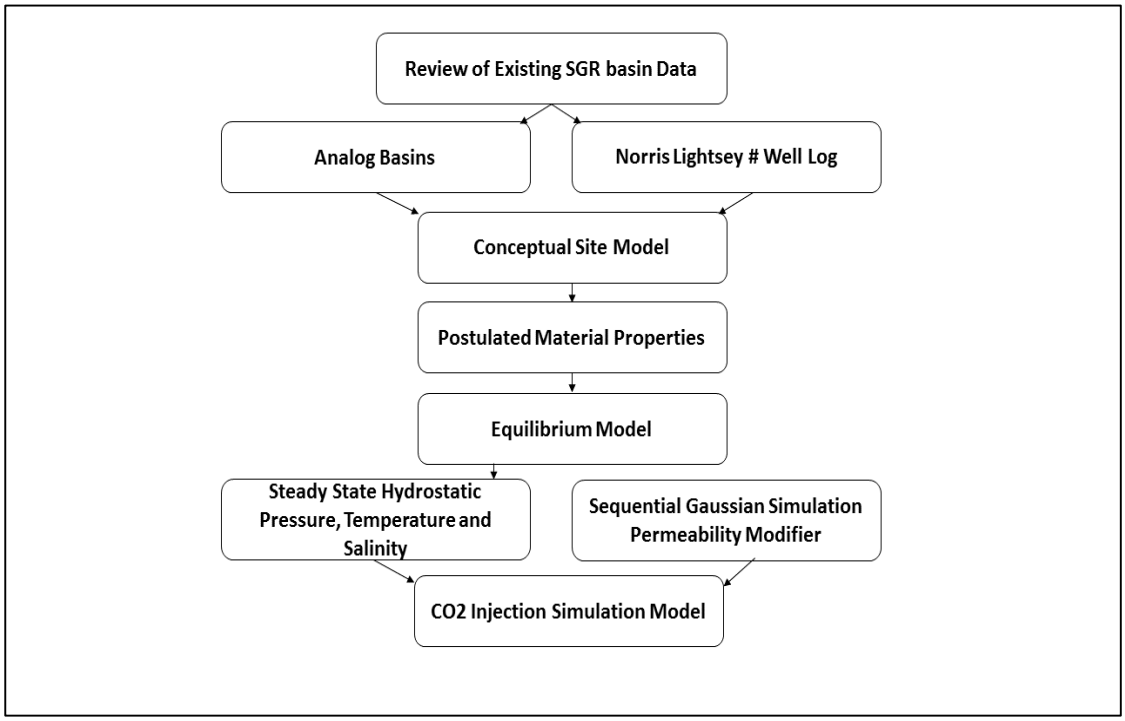

Table 2.2 Results of the equilibrium model showing hydrostatic pressure vs. depth considering temperature and salinity for every 10 horizons within the full vertical dimension of the domain.

Layer	Top	Bottom	Pressure, Pa	Temperature Degrees C	Salt Mass Fraction
1	0	-40	97981	15.5	5.20E-05
10	-360	-400	3618651	24.5	1.07E-04
20	-760	-800	7508566	34.5	2.38E-04
30	-1160	-1200	11366485	44.5	5.29E-04
40	-1560	-1600	15185285	54.5	1.18E-03
50	-1960	-2000	18960265	64.5	2.62E-03
60	-2339.95	-2400	22598440	74.25	5.69E-03
70	-2760	-2800	26391763	84.5	1.28E-02
80	-3160	-3200	30112647	94.5	2.81E-02
90	-3534	-3582	33769369	103.95	5.80E-02
100	-3944.66	-4000	38539006	114.31	1.24E-01

Table 2.3 Material Properties of the three major rock types used in the injection simulation. Sources include Norris Lightsey #1 well log, relevant literature and TOUGH2 Manual default data for material type.

Property	Units	Coastal Plain	Reservoir	Seal
XY Permeability	m^2/mD	3.60e-12/3650	9.87e-15/10	1.00e-20/1.00e-5
Z Permeability	m^2/mD	3.60e-13/365	9.87e-15/10	1.00e-20/1.00e-5
Porosity	%	20	6	0.1
Rock Density	kg/m^3	2,400	2700	2,933
Corey S_{gr}	-	0.05	0.05	0.05
Corey S_{lr}	-	0.17	0.15	0.20
van Genuchten P_o	kPa	2.10	1.50	337.00
van Genuchten λ	-	0.46	0.46	0.46
van Genuchten S_{lr}	-	0.17	0.15	0.20

Table 2.4 Parameters that varied to experiment with different modeling scenarios.

Parameters that were varied		
Material	**Porosity Range (%)**	**XY Permeability (mD)**
Reservoir	0.01 - 0.25	1 mD - 1000 mD
Sill	0.001 - 0.25	0.00001 mD - 1000 mD
Solution Controls	Years	
Injection Time	30 - 1000	
Shut-in Time	0 - 9,700	
End time	30 - 10,000	

Table 2.5 Maximum pressure at the well head as a result of CO_2 injection at a rate of 1 million tonnes per year for 30 years. Lithostatic pressure at the injection depth is ~ 65 MPa.

Time Step (yrs)	Maximum Pressure (MPa)	Injection Horizon Litho-Static Pressure (MPa)
3.1688E-08	32.49	~65.00
1	32.49023	~65.00
5	32.49545322	~65.00
10	32.499372	~65.00
15	32.5013673	~65.00
20	32.61847671	~65.00
25	33.8951342	~65.00
30	34.9798193	~65.00
40	34.21795855	~65.00
50	34.25720533	~65.00
60	34.18094097	~65.00
70	34.11525042	~65.00
80	34.05397069	~65.00
90	34.04202138	~65.00
100	33.98237462	~65.00
250	33.08928793	~65.00
500	32.60085565	~65.00

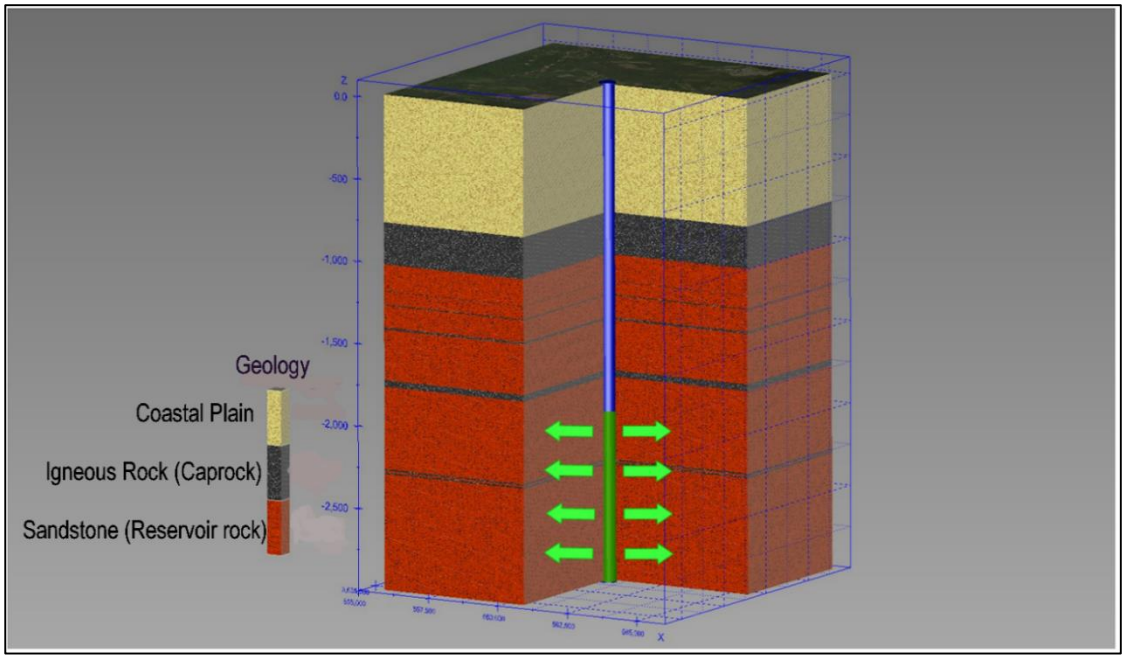

Figure 2.1: Conceptual solid earth model for the South Georgia Rift Basin. The light brown represents the unconsolidated coastal plain sediments, the red represent the sandstone reservoir material, and the dark gray represents the diabase seals. The green represents the base of the injection well and the stacked series of injection zones.

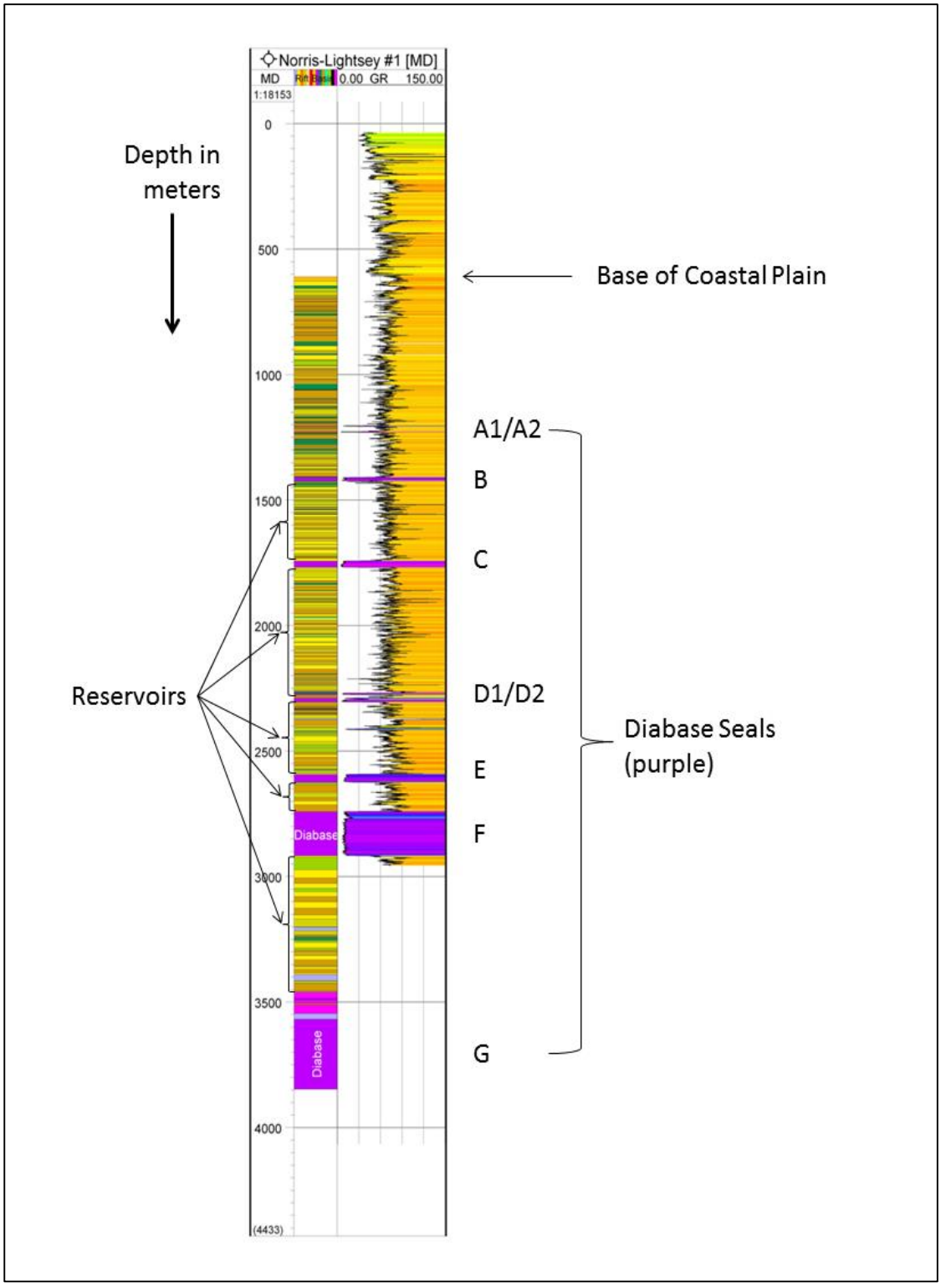

Figure 2.2: Norris Lightsey #1 litho-stratigraphic well log with Gamma. Injection simulation took place in the reservoir between Diabase E and Diabase F.

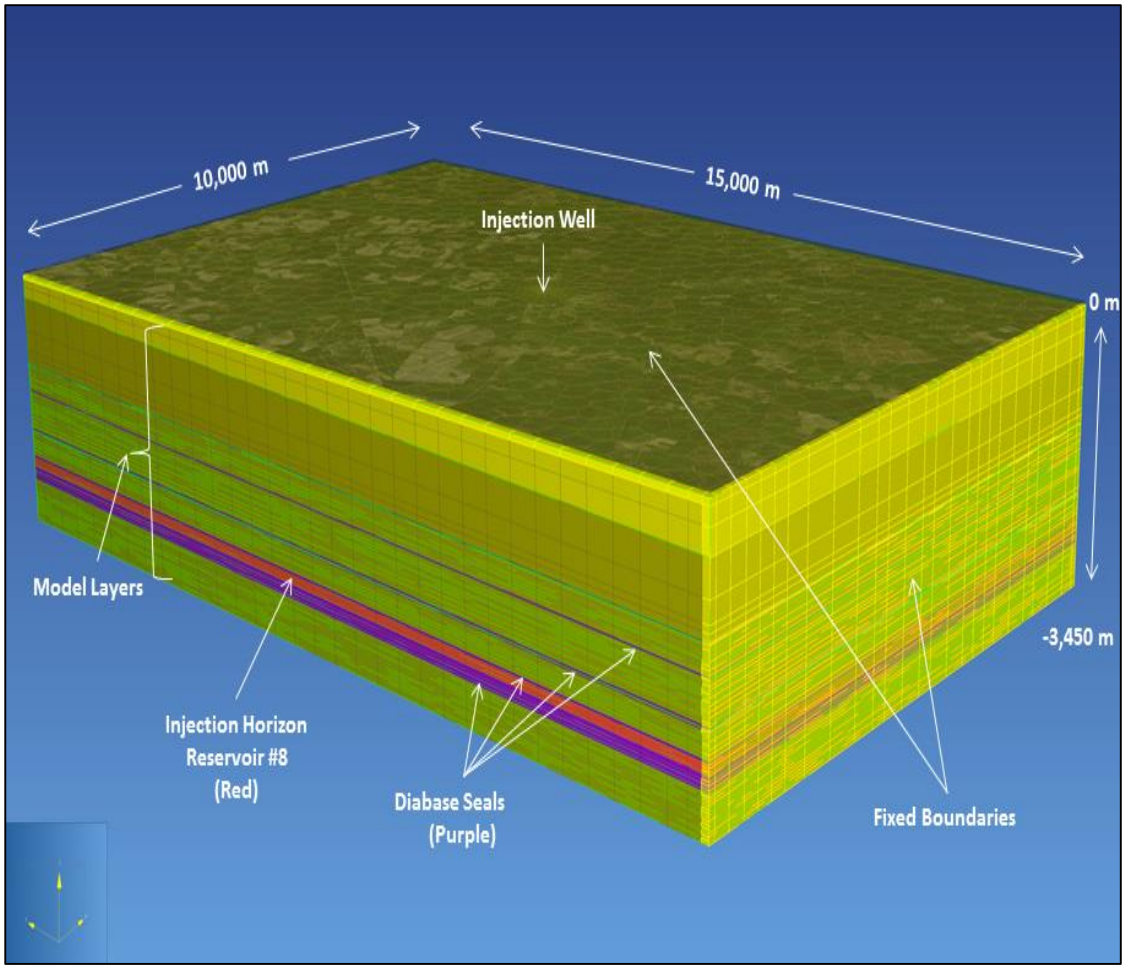

Figure 2.3: CO_2 injection simulation model domain based on Norris Lightsey #1 well lithology. The simulated injection well is located coincidently with the Norris Lightsey #1 well location and injection simulation will take place in red horizon. (between Diabase E and Diabase F in Figure 2.2).

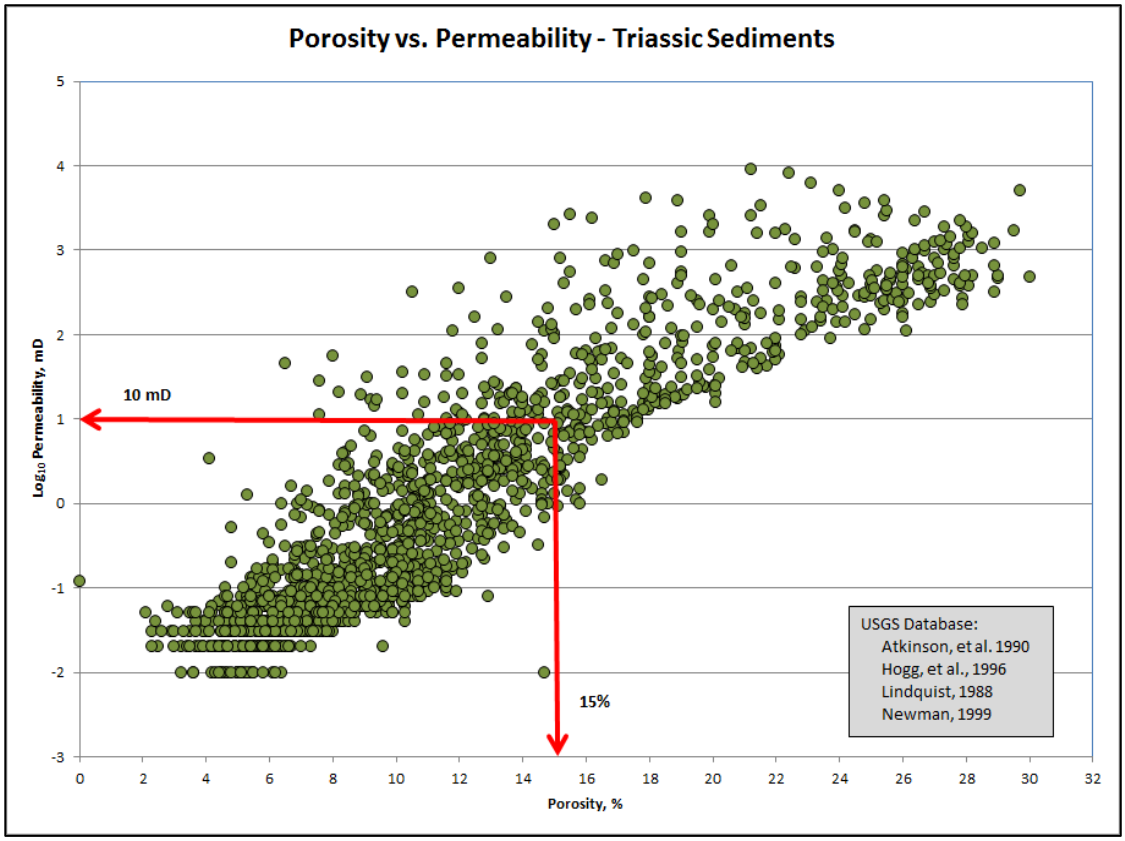

Figure 2.4: Scatterplot of USGS international database of porosity and permeability of Triassic Sediments. The mean porosity and permeability was used to postulate the reservoir data. Source: USGS Open-file Report 03-420.

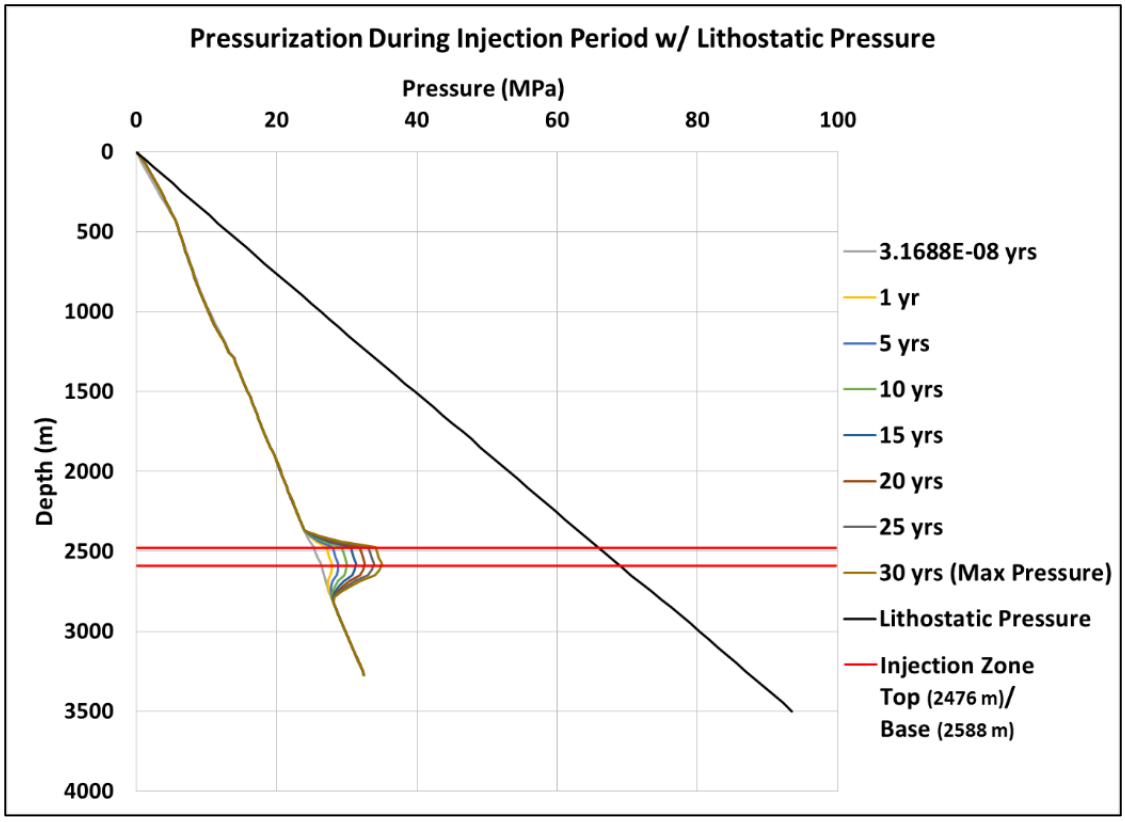

Figure 2.5: Pressure buildup adjacent to the injection well during injection compared to the lithostatic pressure (black line). Injection rate is 1 million tonnes of CO_2 per year for 30 years.

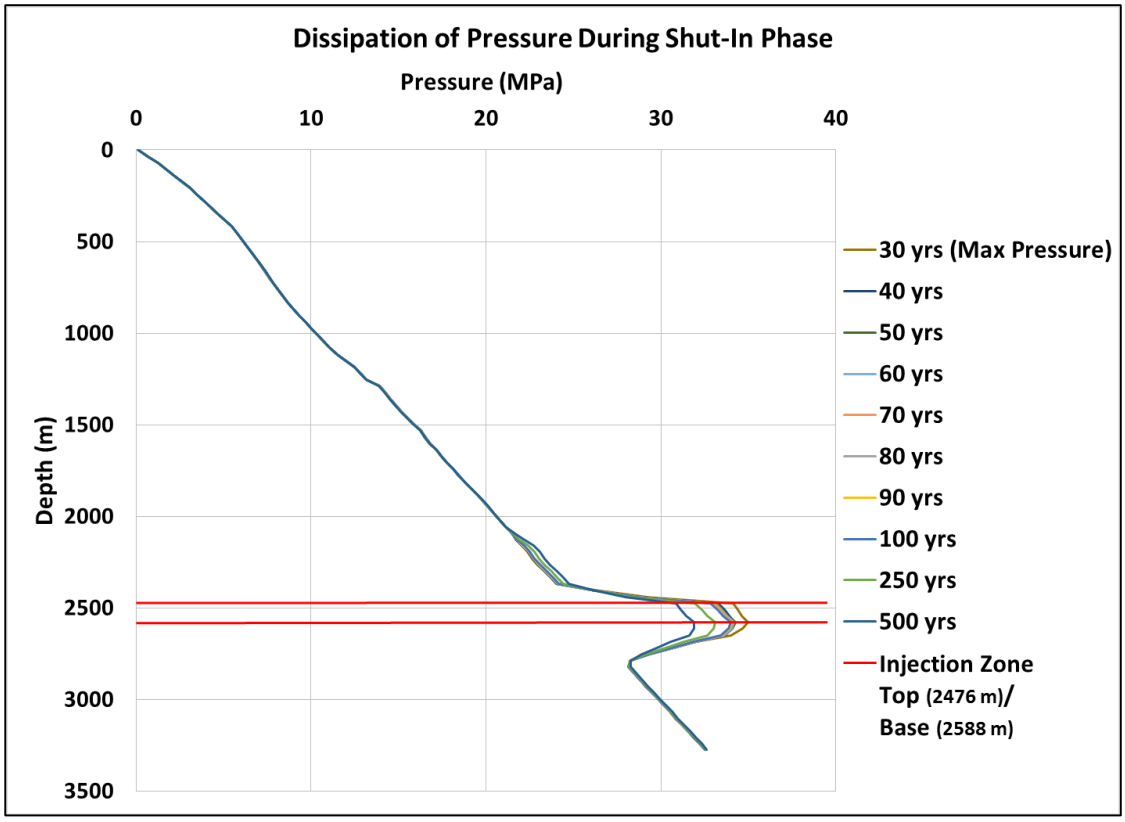

Figure 2.6: Pressure buildup adjacent to the injection well during injection. Injection rate is 1 million tonnes of CO_2 per year for 30 years

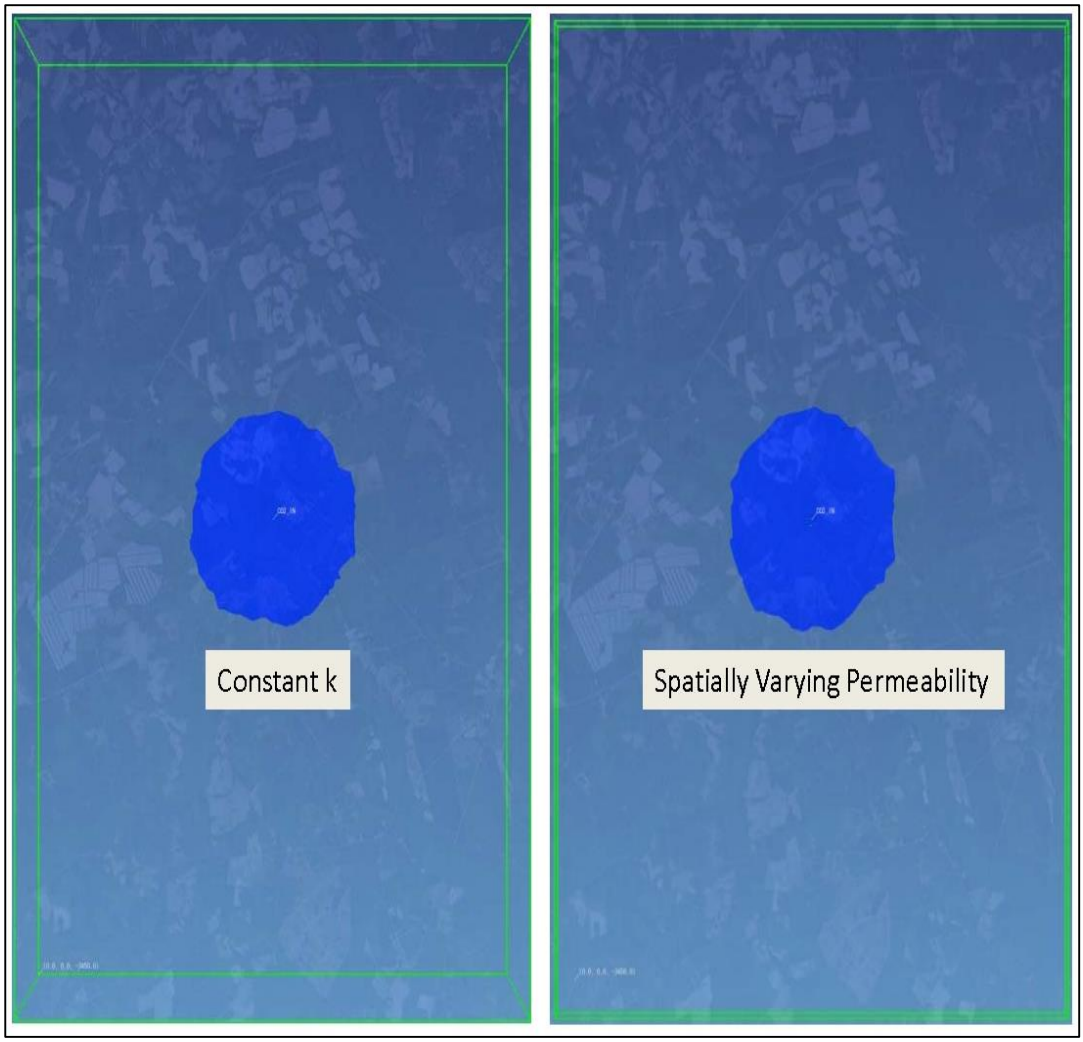

Figure 2.7: Effect of uncertainty in permeability heterogeneity in the injection reservoir on CO_2 plume footprint after 1,000 year simulation with 30 years injection of 1 million tonnes CO_2 and 970 years of shut-in. Left image assumes homogeneous conditions with a constant k (10 mD) while the right image shows the results of the same simulation with a k modifier ranging from 10 mD to 100 mD.

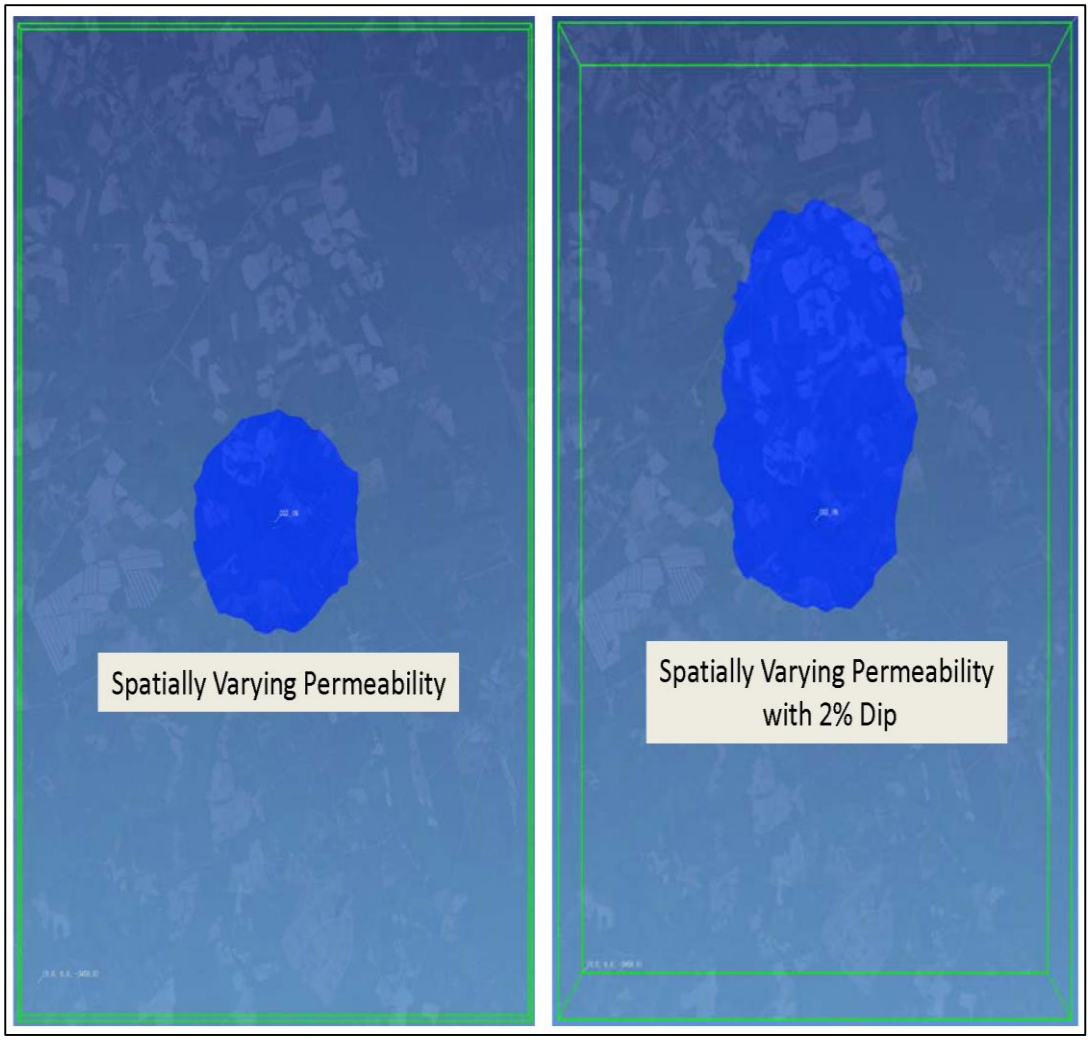

Figure 2.8: Effect of geologic structure (2% northward oriented dip) on CO_2 plume footprint after 1,000 year simulation with 30 years injection of 1 million tonnes CO_2 and 970 years of shut-in. Left image shows the results of the simulation with a spatially k in the range 10 mD to 100 mD but no dip. The right image shows the up-dip migration of the CO_2 plume as a result of the 2% dip in the reservoir strata.

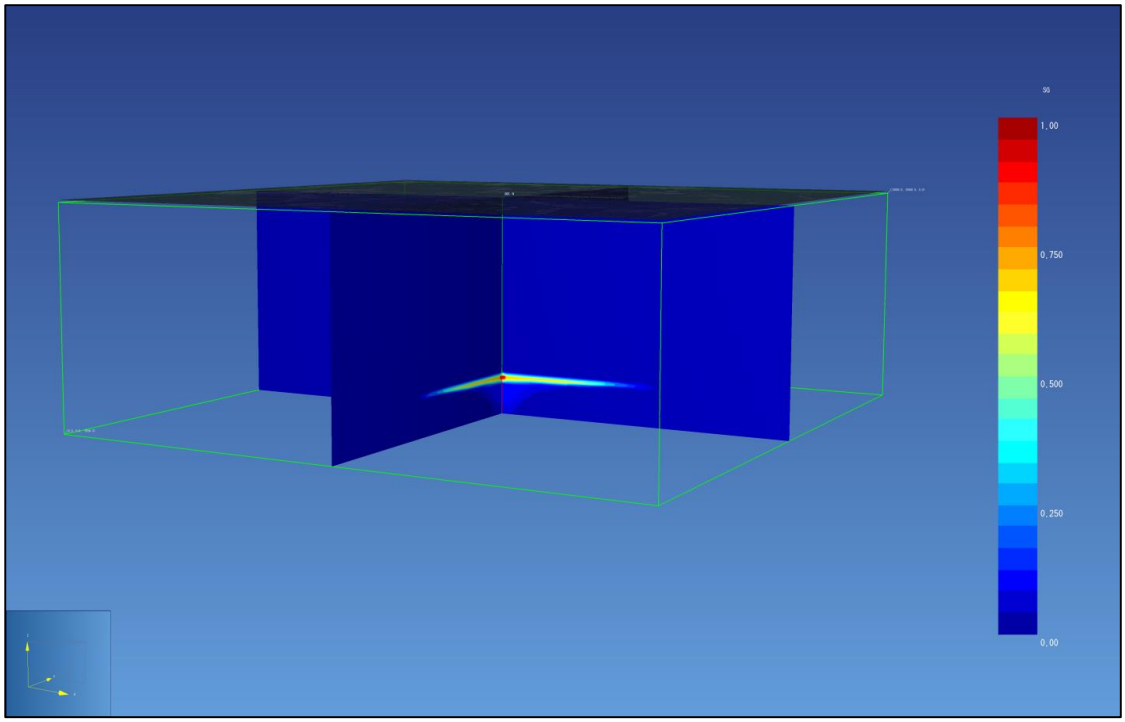

Figure 2.9: Results of simulation of 1 million tonnes CO_2 injection per year for 30 years after 1000 years (i.e., 970 years of no injection).

Chapter 3

Inclusion of Faults in 3-D Numerical Simulation of CO_2 Injection into the South Georgia Rift Basin

3.1 South Georgia Rift Geology - Newly Acquired Data

The previously described SGR basin characterization study catalogued numerous geological, geophysical and petrophysical research (Akintunde *et al.,* 2012; Akintude *et al*., 2013; Brantley *et al*., 2015; Clendenin *et al.,* 2011; Clendenin, 2013; Heffner *et al.*, 2011; Heffner, 2013; Hollon *et al.,* 2014; Rine *et al.,* 2014; Shafer and Brantley, 2011; Waddell *et al.,* 2011; Waddell *et al*., 2014). During the second phase of the characterization study, approximately 386 km (~240 mi) of seismic data were collected, processed and interpreted. During the third phase of the project, the characterization borehole Rizer # 1 was drilled to a depth of approximately 1,889 m (~ 6,200 ft.) Cores from this borehole were sent to Weatherford® Laboratories for petrophysical analyses. The results from the Weatherford® Laboratories analyses indicate that the SGR basin was once buried up to 5 km (3.1 mi) deeper than previously believed. At that depth, the target reservoir (Diabase C) would have been buried up 7,750 m (25,427 ft.) deep (Rine *et al.* 2014). Due to the depth of the burial of the sandstone, there was significantly more compression of the material than was previously thought before the characterization study. For this reason, the postulated porosity and

permeability (6% and 10 – 100 mD respectively) data used in phase one of the injection simulation modeling were significantly over estimated. Newly analyzed data suggest average ambient porosities for rotary and conventional core samples are 3.4% and 3.1%, respectively, and average permeability of rotary air and conventional core samples are between 0.065 millidarcy (mD) and 0.0049 mD, respectively. These values of porosity and permeability values are markedly different than this used in the phase one study.

Using the newly acquired petrophysical data, along with the newly acquired seismic data, a 3-D geologic model of the study was created using Petrel™ (Figure 3.1). The results of the SGR basin characterization study have drastically changed what was once thought about the SGR basin, in particular, about the efficacy of using the Triassic sandstone horizons for permanent geologic storage of supercritical CO_2.

3.2 Research Objectives

Using newly acquired seismic and borehole geophysics data, phase two of the injection simulation modeling created a more realistic CO_2 injection simulation model for the SGR basin as compared to our previous study, phase one. For phase two, an entirely new domain (compared to that in phase one of the modeling) was created using: 1) The 3-D grid from Petrel™ that includes interpreted basin structure and 2) Parameterization using SGR basin material data derived from petrophysical analyses and the newly acquired Rizer #1 characterization borehole geophysical logs. Rizer # 1 is a characterization borehole drilled to validate the

newly acquired seismic data as well as to correlate to horizons evident in the N.L. # 1 well. The 3-D geologic model created in Petrel™ provides a refined stratigraphic, volumetric and structural domain that includes faults. This geologic model along with the empirically derived material data provided by Weatherford® Laboratories, allowed us to create an injection simulation model realistic to SGR basin conditions than the phase one modeling effort, which was mostly parameterized using basin data based on literature and the N.L. # 1 well log. Research done by Rutqvust et al. (2007) suggests faults, fractures and deteriorated abandoned drill holes or wells comprise primary risk factors for leakage in engineered CO_2 injection systems. Corroborating this finding, Deng et al. (2012) concluded that risk assessments of potential sequestration site leakage should consider faults and fracture zones to evaluate the potential for premature failure of a designed system. Faults can either serve as high permeability by-pass conduits that allow CO_2 to escape out of the target reservoir or they can act as low permeability seals that can aid in the compartmentalization of CO_2 in the target reservoir. In this work, we estimated a permeability range within the faults based on the Rizer # 1 borehole geophysical logs and used this range to investigate the impact of faults on the flow of supercritical CO_2 into the fractured and faulted diabase injection zone. The goal of these simulations were to: 1) Create a new dynamic model of the SGR basin for CO_2 injection simulation; 2) Analyze the effects of fractures and faulting in the injection reservoir and seal geology, and 3) Test the feasibility of the SGR basin for the long term storage of 30 million tonnes of supercritical CO_2.

The long term fate of injected CO_2 for geologic storage is divided into four different storage modes: 1) Free gas; 2) Trapped gas; 3) Dissolved in the formation brine; and 4) Gas sequestered as solid minerals or mineralization trapping. Modes 1, 2 and 3 can be simulated with multiphase flow simulators such as TOUGH2-ECO2N (Pruess 2005, Hou, 2012, Brantley et al., 2015, Zhang et al., 2011; Omambia and Li, 2010) and CMG-GEM (Basbug and Gumrah, 2005, Frangeul et al., 2004). However, the mineralization trapping can only be simulated using a reactive transport model (Shu et al., 2012; Thibeau and Nghiem, 2007). In this study, we focused on the first, second and third modes using the multiphase simulator CMG-GEM. GEM is the Computer Modeling Group's (CMG) Generalized equation-of-state Model (GEM) compositional simulator which includes options such as CO_2, miscible gases, volatile oil, gas condensate, horizontal wells, well management, complex phase behavior among others (http://www.cmgl.ca/software/gem2014, GEM2014.10, 2014.).

3.3 Injection Simulation Modeling

The complexity of the SGR basin structure presented a challenge in developing the 3-D geologic model in Petrel™. The only units that could be mapped between the Rizer #1 borehole and the N.L. # 1 borehole are the diabase intrusive units. The N.L. # 1 boring log indicates sequences of sandstone, diabase, and shale and was used to correlate with the newly acquired seismic and borehole data to help produce the 3-D geologic model. The complexity of the structure made correlation between sandstone units almost impossible. The following horizons were mapped:

base of the Coastal Plain, the top and base of diabase units C, E, and F (Figure 3.2). The results from the petrographic and core analyses ruled out using the sandstone as possible injection zones due to its aforementioned low porosity and permeability (3.1% and 0.065 mD). The only possible porous zones that could be used for CO_2 storage and injection simulation are along the diabase units. These diabase units are highly fractured and the Rizer #1 geophysical log indicates the average porosity to be approximately 10% and the average permeability to be approximately 10 mD. During the drilling of Rizer # 1, water flowed into the borehole from one of the diabase horizons and this empirically supports the log data that the diabase is highly fractured.

For phase two of the injection simulation modeling, two software packages were employed to build the injection simulation model. Petrel™ was used to construct a geo-cellular grid based on the 3-D geologic model. CO_2 injection simulation was achieved using the compositional reservoir simulator CMG-GEM (Delshad et al., 2010; Saadatpoor et al., 2009). The geologic horizons were created in Petrel™. These horizons were then imported into CMG-GEM as isopachs.

The model volume used in all of the phase two simulations is 178 x 142 x 50 (i, j, k) for a total of 1,167,563 active cells. The typical cell size is 100m x 100m x 200m. However, there was grid refinement of the injection horizon surrounding the injection well and k values varied by the thickness of the horizon. Adjacent to the well, an area of 5 (x direction) x 6 (y direction) cells (500 m x 600 m) was refined into 3 (i) x 3 (j) x 1 (k) for a total of 2,700 refined cells for each layer in the model.

Grid refinement is used to allow for the incorporation of greater spatial information in a computationally efficient way, thus creating a hierarchical concept of space around the injection well (Brantley et al., 2015). The k (vertical) cells varied in thickness along with the horizon surfaces were divided into 50 layers as follows (Figure 3.3; Table 3.1):

Layers 1 to 10: Diabase C

Layers 11 to 20: Sandstone 1

Layers 21 to 30: Diabase E

Layers 31 to 40: Sandstone 2

Layers 41 to 50: Diabase F

In order to optimize the computation efficiency of the model, only the horizons below the coastal plain were used in the simulation modeling. These include Diabase C, Sandstone1, Diabase E, Sandstone 2, and Diabase F. CO_2 was injected into Diabase E and Sandstone 1 is assumed the caprock seal.

Material properties were assigned based on the Weatherford® Laboratories results and the Rizer # 1 petrophysical ELAN logs. All of the diabase horizons were assigned a porosity of 10% and a heterogeneous permeability distribution as shown in Figure 3.4. The permeability heterogeneity was generated by specifying a random permeability between 1 and 100 mD. The scale is logarithmic so the actual data is a random number between >0 and 2. This range was estimated based on the fractured nature of the diabase evidenced by the Rizer #1

petrophysical ELAN logs. All sedimentary horizons in the model serve as caprock due to their low permeability and porosity. They are given a vertical and horizontal permeability of 0.065 mD and porosity of 3.4%. The simulation model parameters along with the horizon surfaces minimum and maximum depths are shown in Table 3.1. As with the preliminary model (phase one), 30 million tonnes of CO_2 were injected at a rate of 1 million tonnes per year (1.38E7 m^3 per year), which is the DOE's stated minimum capacity to be considered a viable basin for geologic storage. Model complexity resulted in a significant amount of computer time to reach convergence. For this reason, we chose 100-year simulations for Phase two of the modeling. As with Phase one, the first 30 years were injection of supercritical CO_2. However, instead of a 970 year shut-in as with phase one, there was only a 70-year shut-in with Phase two because of simulation time requirements. The first year of the simulation (1/1/2014 – 12/31/2014) was used as time for model equilibration. Injection of supercritical CO_2 started on 1/1/2015 and continued until year 2045 and shut-in spanned 2045 – 2115. The maximum time step was set to 30 days although this was rarely reached due to the complexity of the geology.

3.4 CO_2 Injection Results

To examine the impact of potential fault leakage, numerical simulations were conducted using a progressively higher permeability in the faults zones identified in the 3-D geologic model. For the first experiment, a permeability of 0 mD was assigned to the faults. In this scenario, the faults serve as seals. As expected, the CO_2 was contained in the injection zone Diabase E and there was no CO_2 leakage

or migration out of the target reservoir for the entire 100-year numerical experiment. Figure 3.5 is a 2-D image of the CO_2 saturation of the top layer of Diabase E (layer 21 in the model) and shows the areal extent of the CO_2 plume. Figure 3.6 plots the dissolved phase CO_2 against the supercritical CO_2. The CO_2 is dissolving the fastest during the 30-year injection phase and this slows as soon as the injection stops. However, CO_2 continues to dissolve for the entire 100-year experiment - this is important because dissolution into the host brine is the third trapping mechanism of CO_2 in geologic storage. This is corroborated by the supercritical CO_2 plot peaking at the end of the injection period and then trending in a steady decline as more CO_2 dissolves into the brine.

For the second numerical experiment, a permeability of 1 mD was assigned to the faults. This scenario represents a leaky fault with small interconnected fractures. This scenario is significant because a low permeability like 1 mD may not be viewed as a significant source of leakage. Figure 3.7 shows the top of Diabase E (layer 21 of the model) and the 2-D areal extent of the CO_2 plume migration at the top of the injection horizon. It closely resembles the plume extent in Figure 3.5. These plumes resemble each other in the 2-D view because the amount of leakage up the 1 mD fault was 47% of the total volume of injected CO_2 (Table 3.2), therefore 53% of the CO_2 is trapped by the caprock and pooled in the top of the injection horizon. However as is shown in Figure 3.8, even at permeability as low as 1 mD causes significant leakage (~ 47% of the total injected CO_2) and upward migration of CO_2 out of the target reservoir. Figure 3.8 is a 3-D image of the CO_2 migration over the 100-year simulation. As can be seen in Figure

3.8, the CO_2 migrates up the faults and pools in Diabase C, which is the top boundary of the model. Given the injection depth of [(~1710 m – 2953 m; 5610 ft. – 9688 ft. (Table 3.1)] and the 100 year time scale, the CO_2 transport is mainly due to buoyancy and dispersion, not advection. The injected CO_2 has a specific gravity at the injection depth of approximately 0.7 (Mammoli and Brebbia, 2011). Therefore, due to buoyancy, the CO_2 will rise in the more dense brine occupying the pore space. This can be seen in Figure 3.8 as the CO_2 follows the contours up dip in the formation and pools up against the bottom of the caprock as well as traveling up the permeable faults and pooling at the top boundary of the model.

For the final numerical experiment, a permeability of 100 mD was assigned to the faults. This experiment represents a highly fractured fault zone with a high leakage rate. Figure 3.9 is a 2-D image of the areal extent of the plume at the top of the model in Diabase C. This image shows that much of the CO_2 has migrated up the fault and pooling in high concentrations in the top layer of the model. Figure 3.10 is a 3-D image of CO_2 saturation after 100 year simulation with the fault permeability set to 100 mD. This image better displays the amount of CO_2 that has traveled up the fault out of the target reservoir of Diabase E and into Diabase C. This is significant because it illustrates that a fault with 100 mD permeability is a large conduit and CO_2 will escape at a very rapid rate on a human time scale. In the 100 year simulation, ~85% of the CO_2 injected migrated up to the top of the model (Table 3.2; Figure 3.11).

It was determined that at injection depth, the lithostatic pressure ranges from ~60 – 65 MPa. The maximum injection pressure is ~31 MPa, which is

approximately half of the lithostatic pressure in the injection zone (Figure 3.12) thus indicating injecting activity would not induce seismicity and further fracturing.

The results from this research illustrate that even with a permeability of 1 mD significant leakage and migration of CO_2 occurs up faults (Table 3.2). Figure 3.12 graphically compares the volume (m^3) of CO_2 that remained in the target reservoir with the fault permeabilities set to 1 mD and 100 mD. This graph makes it easier to visualize, conceptualize and compare the amount of CO_2 that was injected versus the amount of CO_2 that remained in the target reservoir. This is evidence that fault analysis can be a critical factor in injection simulation modeling and ultimately in determining the efficacy of long term geologic storage of CO_2 and that even low permeability faults make the geology potentially unsuitable.

3.5 Tables and Figures:

Table 3.1. Injection simulation model domain information.

Injection Simulation Model Set Up					
Material	**50 Layers Total in the Model**	**Depth (m)**	**Porosity (%)**	**Permeability (mD)**	**Notes**
Diabase C	Surface Top Layer 1	Minimum 1283 m			
	Surface Bottom Layer 10	Maximum 1916	10.0%	10 mD	Top of the Model
Sandstone 1	Surface Top Layer 11	Minimum 1387 m			
	Surface Bottom Layer 20	Maximum 2848 m	3.4%	0.065 mD	Seal
Diabase E	Surface Top Layer 21	Minimum 1710 m			
	Surface Bottom Layer 30	Maximum 2953 m	10.0%	1-200 mD range	Injection Horizon
Sandstone 2	Surface Top Layer 31	Minimum 1710 m			
	Surface Bottom Layer 40	Maximum 3453 m	3.4%	0.065 mD	Seal
Diabase F	Surface Top Layer 41	Minimum 1710 m			
	Surface Bottom Layer 50	Maximum 3517 m	10.0%	10 mD	Base of the Model

Table 3.2. CO_2 volume injected vs leakage analysis for 1 mD and 100 mD faults.

Fault Permeability	**1 mD**	**100 mD**
Total CO_2 Injected (m^3)	1.6432E+10	1.6432E+10
Simulation Time (years)	100	100
CO_2 Remaining in Diabase E (m^3)	7.0634E+09	2.4183E+09
CO_2 Leakage out of Diabase E (m^3)	9.3682E+09	1.4013E+10
Percent of CO_2 Remaining in Diabase E	57.01%	14.72%
Percent of CO_2 Leakage out of Diabase E	42.99%	85.28%
Leakage Rate (m^3 / day)	1.2898E+05	1.9293E+05
Leakage Rate (m^3 / year)	7.8857E+06	1.1796E+07
Injection Rate (m^3 / day)	2.2622E+05	2.2622E+05
Injection Rate (m^3 / year)	1.3831E+07	1.3831E+07

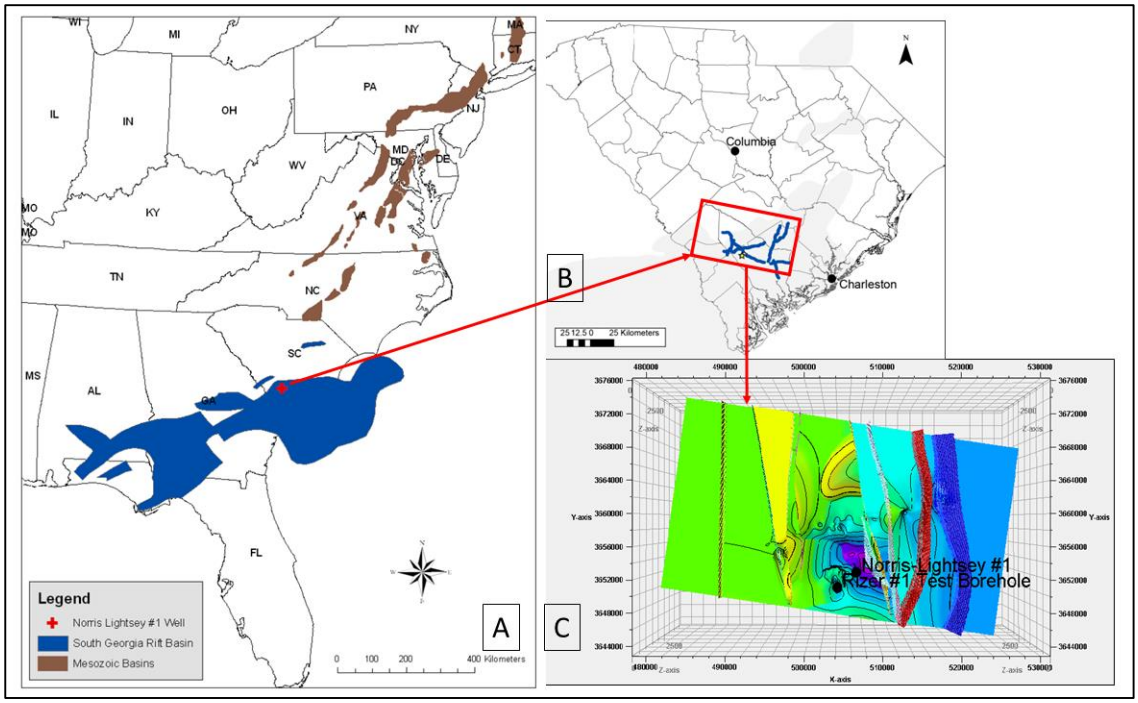

Figure 3.1. Location maps showing the study area and the injection simulation domain boundaries. Map (A) shows the South Georgia Rift basin in relation to the ENARS. Map (B) shows the location of the study area within the SGR basin and map (C) is the top surface, Diabase C, of the 3-D geologic map produced using Petrel™. Color variation indicates the surface depth and various faults.

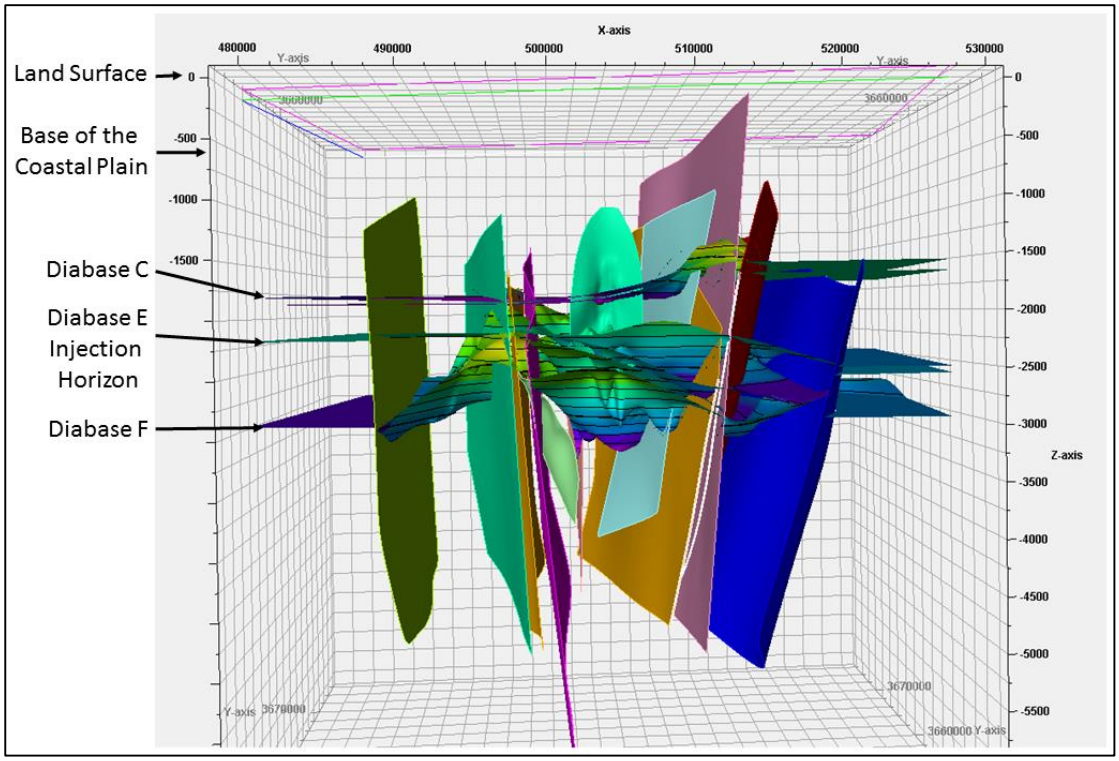

Figure 3.2. Petrel™ produced 3-D geologic model surfaces with the faults. This image illustrates the complexity of the geology and the amount of faulting in the study area. The various colors of each plane represents each individual fault.

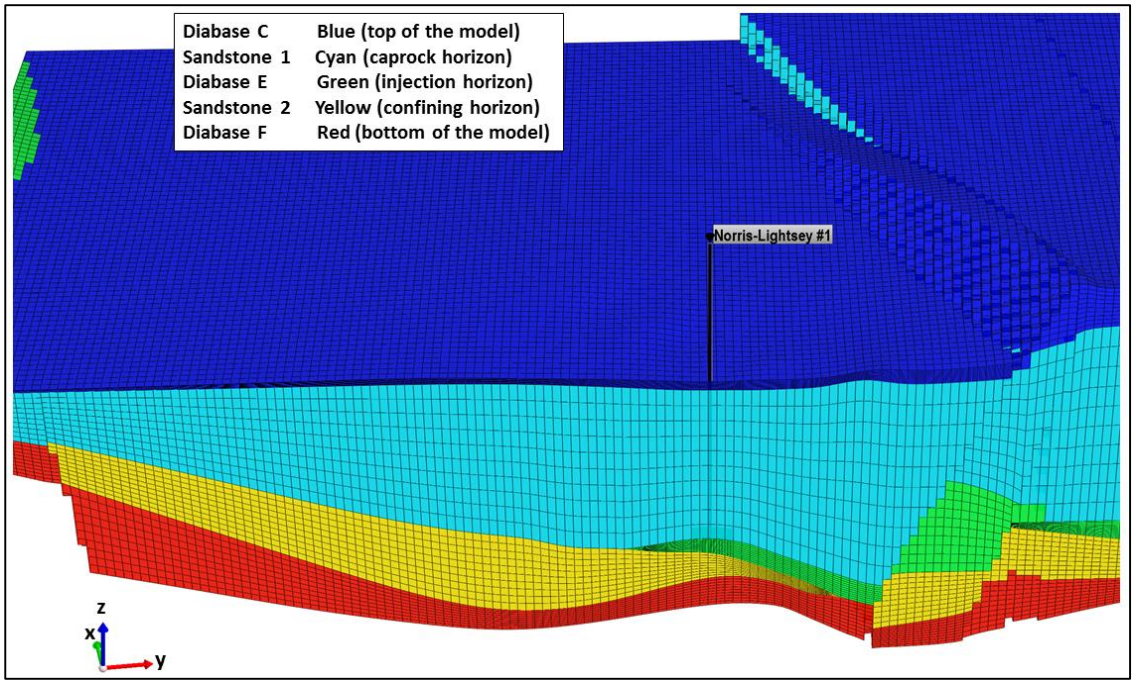

Figure 3.3. 3-D Cross section of the injection simulation model. This image shows the layers and complexity of the geology of the injection simulation model. The top of the model (blue) is Diabase C and is located beneath the Coastal Plain of South Carolina at a depth of ~600 m below land surface. The bottom of the model (red) is Diabase C and has a maximum depth of ~3517 m below land surface.

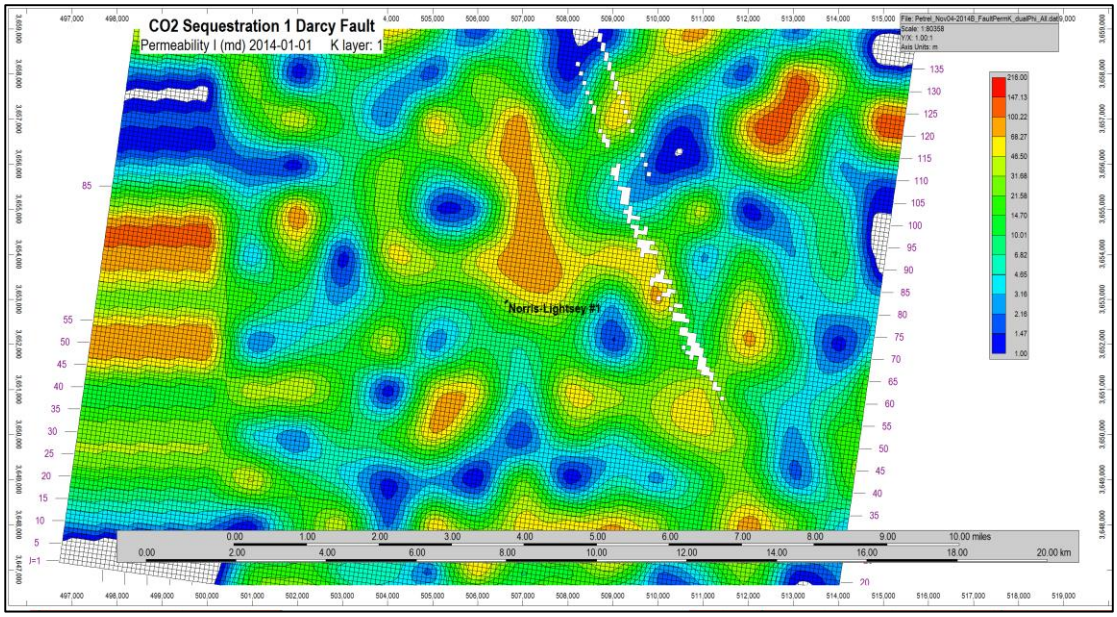

Figure 3.4. Layer 1 (top of the model) permeability distribution. This distribution was used for all of the Diabase layers and ranges in value between 1 and 200 mD. The left side of the permeability map is stretched as a results of the final simulation model grid extending slightly further than the permeability map that was exported from Petrel™. The white diagonal feature is a fault that extends through the top of the model.

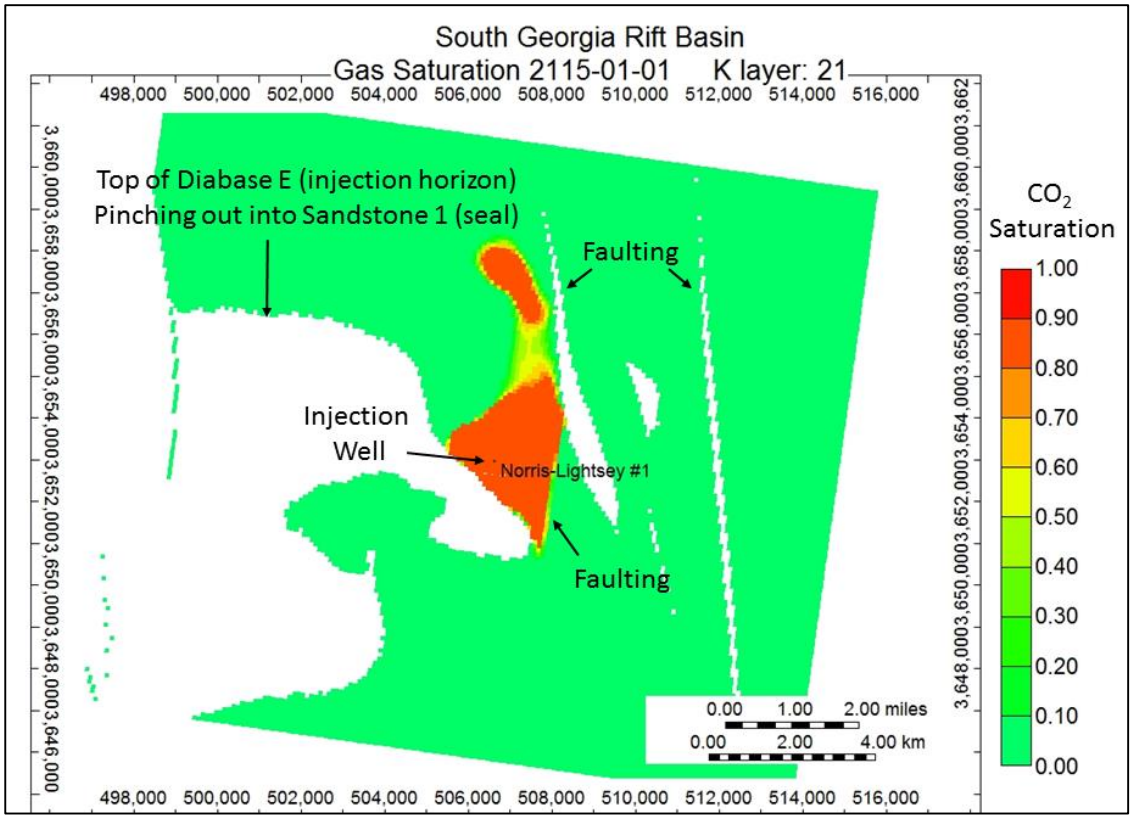

Figure 3.5. 2-D image of CO_2 saturation of the top layer of Diabase E showing the areal extent of the CO_2 plume as a result of 30 millions tonnes of CO_2 injected for 30 years with a 70 year shut-in. In this experiment, the faults permeability was 0 mD and all of the injected CO_2 remained in the target reservoir, Diabase E. This image displays the more buoyant CO_2 rising up the top surface Diabase E and being laterally sealed by the fault and horizontally sealed by Sandstone 1.

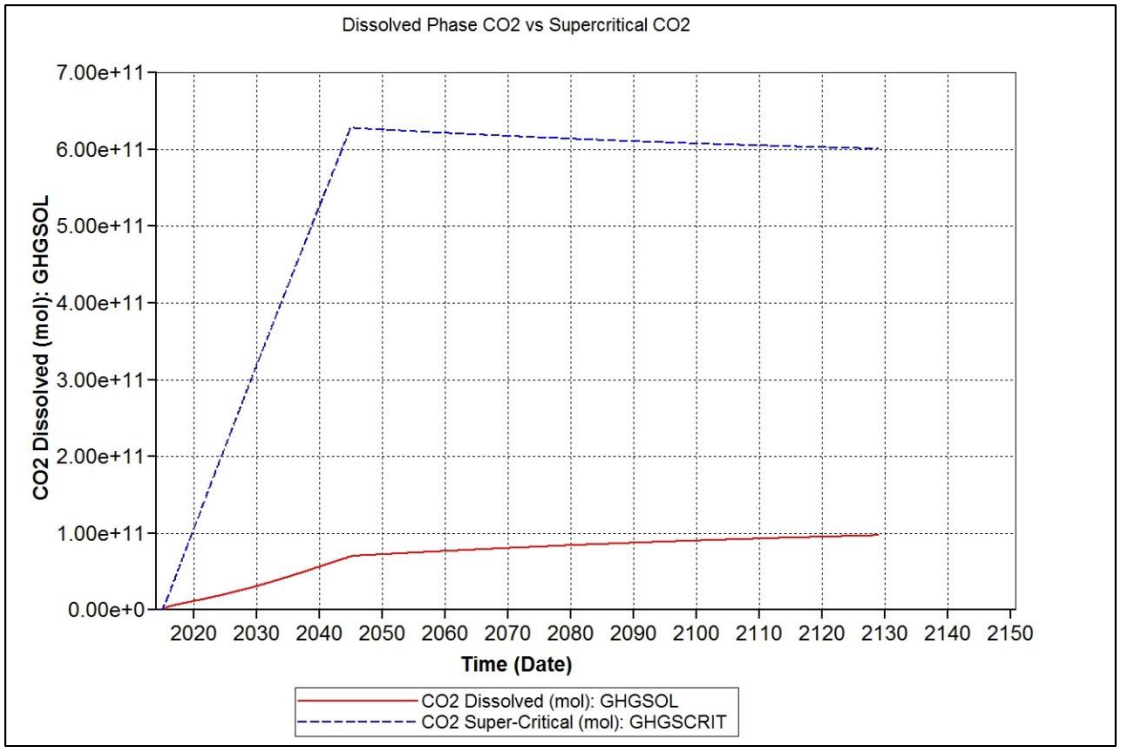

Figure 3.6. Plot of dissolved phase CO_2 vs supercricitical CO_2. In this experiment, the faults permeability was 0 mD and all of the injected CO_2 remained in Diabase E. The injection stopped and shut-in started 1/1/2045. Solubility is a trapping mechanism that begins with injection and can continue until the all of the mechanically or chemically untrapped CO_2 is in solution.

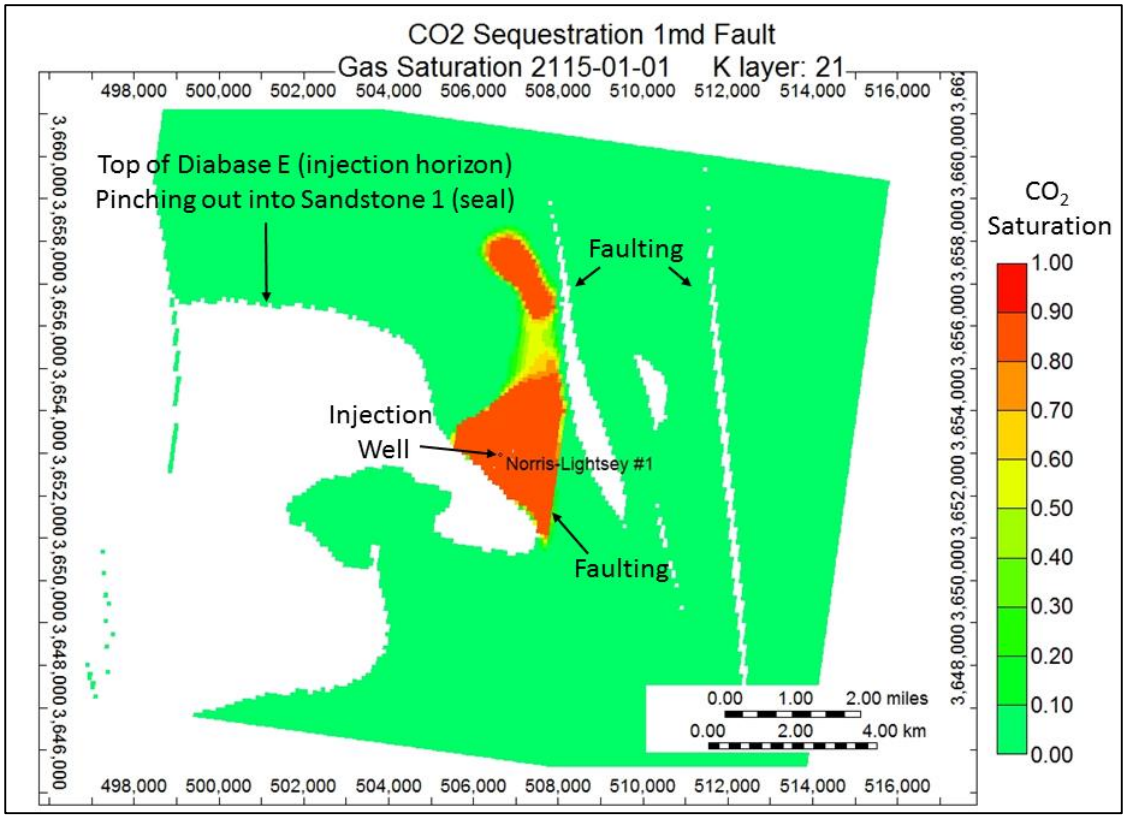

Figure 3.7. 2-D image of the CO_2 saturation of the top layer of Diabase E (layer 21) showing the areal extent of the CO_2 plume as a result of 30 millions tonnes of CO_2 injected for 30 years with a 70 year shut-in with a fault permeability of 1 mD. Leakage out of the target reservoir has happened but it is hard to see in 2-D surface view.

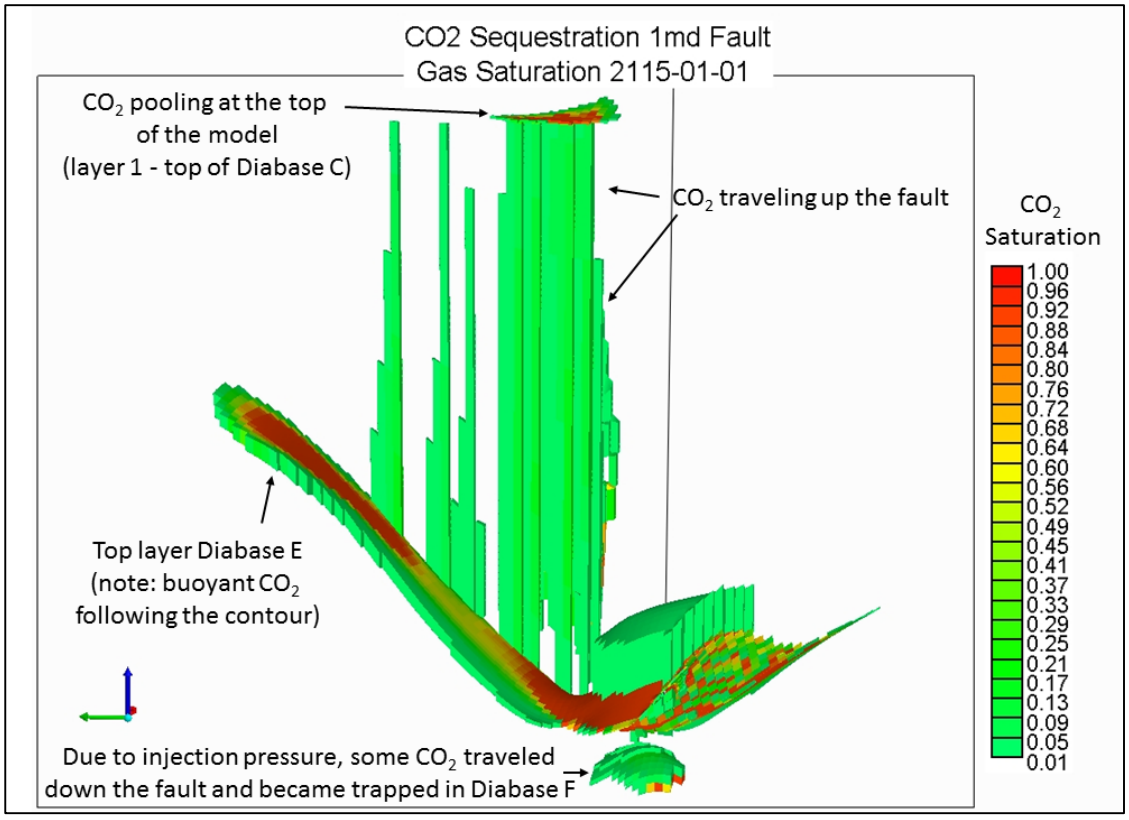

Figure 3.8. 3-D image of CO_2 saturation after 100 year simulation with the fault permeability set to 1 mD. This 3-D image illustrates that: 1) Even with a permeability of 1 mD, there is significant leakeage out of the target reservoir up the faults into Diabase C, which is the top of horizon of the model; and 2) The complexity of the geology. Note the topography of the Diabase C surface.

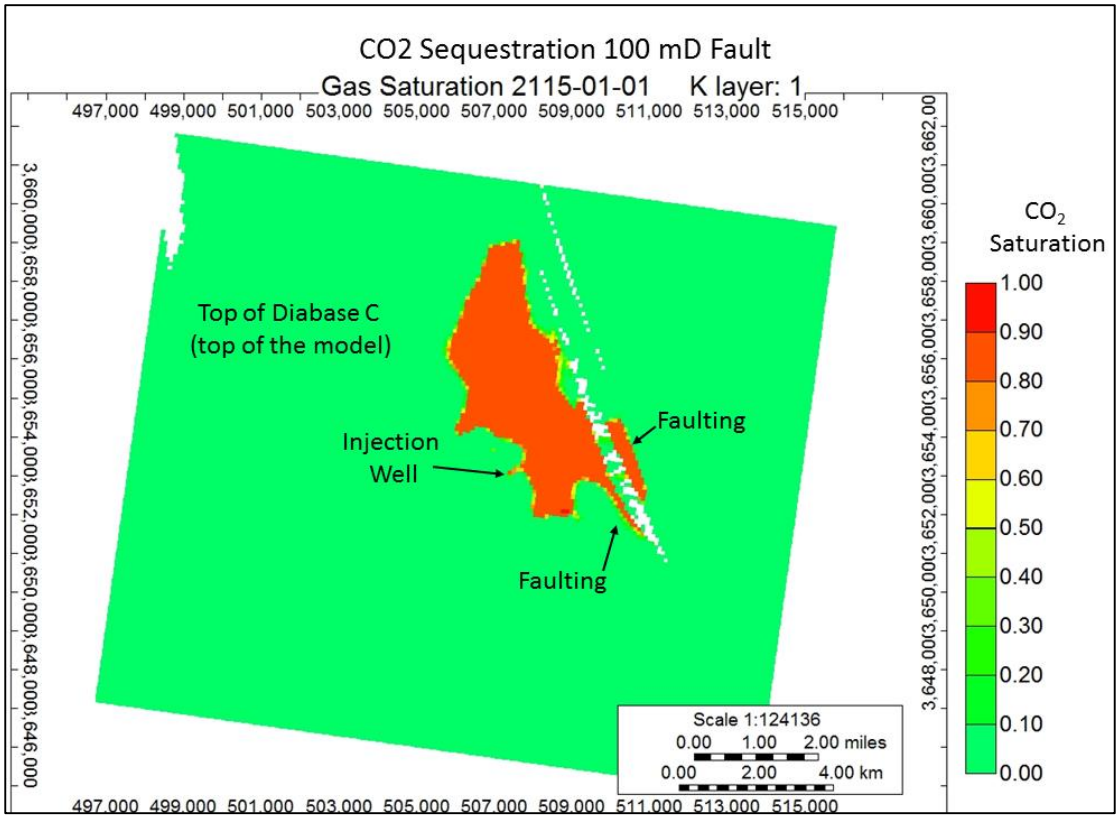

Figure 3.9. Surface image of the CO_2 saturation of the top layer of Diabase C (layer 1) showing the areal extent of the CO_2 plume as a result of 30 millions tonnes of CO_2 injected for 30 years with a 70 year shut-in with a fault permeability of 100 mD. A large portion of the CO_2 has migrated up through the faults into Diabase C, which is the top of the model, and pooled in high concentration.

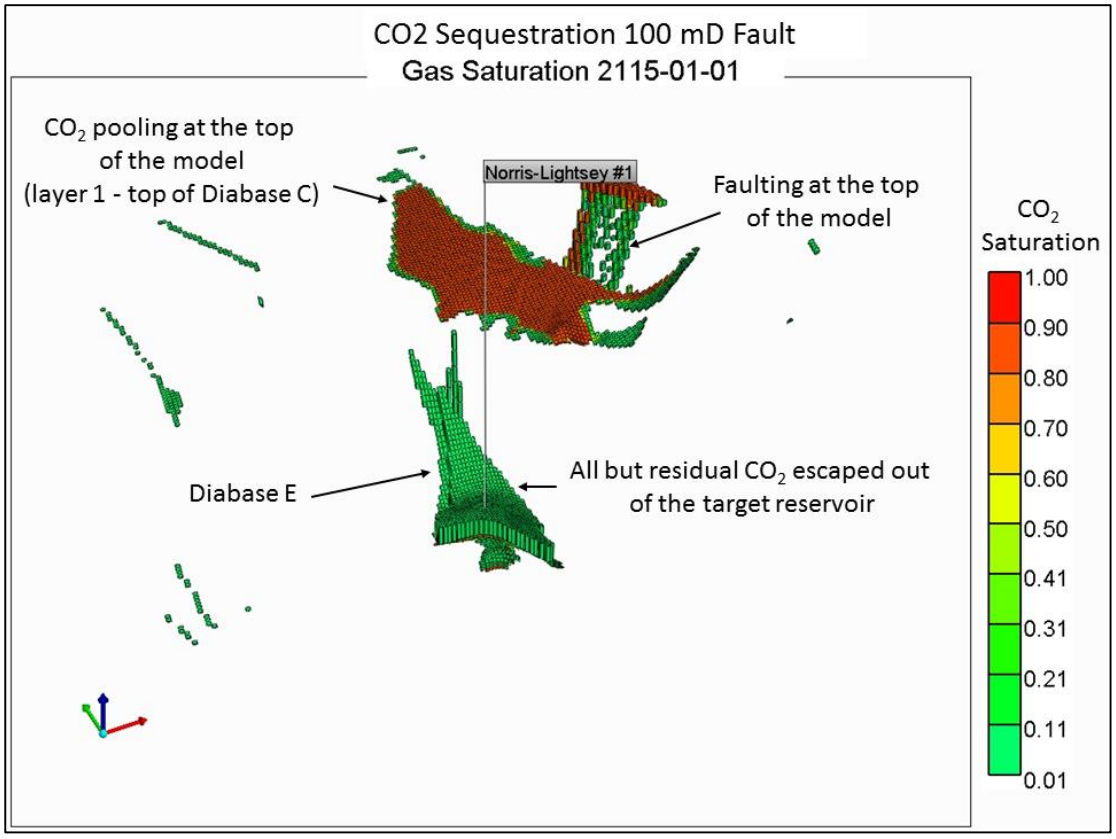

Figure 3.10. 3-D image of CO_2 saturation after 100 year simulation with the fault permeability set to 100 mD. This 3-D image displays (1) significant leakeage up the faults into Diabase C, which is the top of horizon of the model; and (2) the complexity of the geology. In the 100 year simulation, most of the CO_2 injected migrated up to the top of the model pooling in high concentrations.

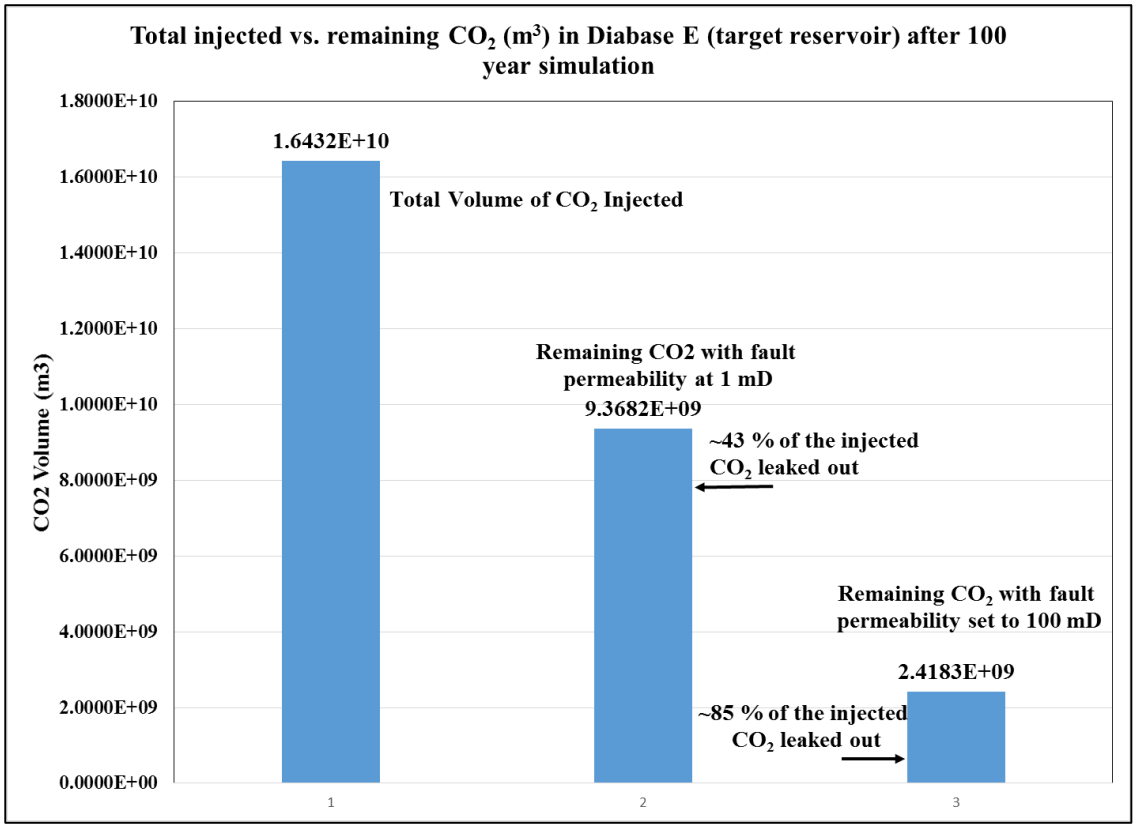

Figure 3.11. Graph of the CO_2 remaining in Diabase E (target reservoir) after the 100 year simulation. The difference between the remaining and total injected is the amount of CO_2 leakage.

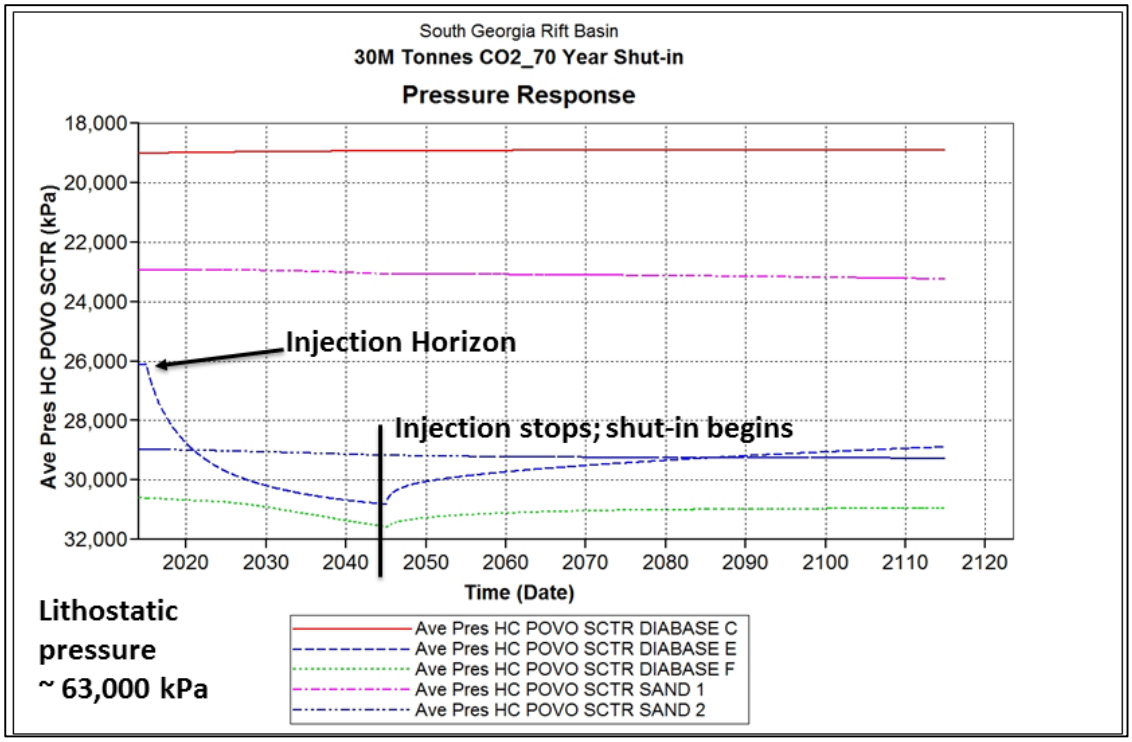

Figure 3.12. Plot of the basin pressure response of each horizon at the injection well. Diabase E (blue dashed line), the injection horizon, has the largest response. Most of the pressure was contained by the Sandstone seal (pink line) above the target reservoir. In this experiment, the faults permeability was 0 and all of the injected CO_2 remained in Diabase E. Note that the maximim injected pressure is below half of the reservoir lithostatic pressure (~63 MPa). HC POVO SCTR is the CMG-GEM software terminology for hydrocarbon pore volume pressure in a particular sector, or in this case CO_2 pore volume pressure in a particular horizon.

Chapter 4

Conclusions and Discussion

4.1 Conclusions

Conclusion of this research are: 1) the SGR basin is composed of numerous sub-basins, 2) this study only looked at portions of one sub-basin, 3) in SC, 30 million tonnes of CO_2 can be injected into the diabase units if the fracture network is continuous through the units, 4) due to the severity of the faulting there is no way of assuring the injected CO_2 will not migrate upward into the overlying Coastal Plain aquifers, and 5) the SGR basin covers area in three states and this project only studied two small areas so there is enormous potential for CO_2 sequestration in other portions of the basin and further research needs to be done to find these areas.

The results from Phase 1 of the injection simulation modeling suggest that the SGR basin is suitable for long term geologic storage of CO_2. However, the results from the more detailed phase two modeling shows the suitability of the SGR basin for long term storage of CO_2 remains inconclusive due to lack accurate data on the fault properties and juxtaposition, given the influence faults may have on CO_2 migration. If the faults act as seals, this portion of the SGR basin is suitable for CO_2 injection using the highly fractured diabase layers as the reservoir horizons and the low porosity and permeability sedimentary sandstone layers as the seals.

However, if the faults have as little as 1 mD of permeability, the seal is compromised and CO_2 will migrate upwards out of the intended reservoir at a rate of 7.8857E+06 m^3 per year, thus deeming this portion of the SGR basin unsuitable for long term geologic storage of CO_2. The results of this study show the importance of:

1) Including accurate geologic structure (particularly faults) into CO_2 injection simulation modeling

2) Knowledge of whether the faults act as leaky conduits or seals

3) Accurate fault permeability data for the containment of CO_2

4) Having correct reservoir data, in particular porosity and permeability for injection simulation modeling.

The results from this research illustrate that even with low permeability faults, significant leakage and migration of CO_2 occurs. This is evidence that fault analysis is a critical factor in injection simulation modeling and ultimately in determining the efficacy of long term geologic storage of CO_2 and that even low permeability faults make the geology potentially unsuitable.

4.2 Discussion

In summary, in the South Carolina (SC) portion of the SGR basin, 30 million tons of CO_2 can be injected into the diabase units if the fracture network is continuous through the units, *however,* due to the severity of the faulting there is no way of assuring the injected CO_2 will not migrate upward into the overlying Coastal Plain aquifers. In SC, the seismic data suggest the faulting extends upward into the

Coastal Plain making that area not suitable for CO_2 storage. The complex faulting observed at the study areas appear to be associated with transfer fault zones (Heffner 2013). Newly acquired seismic data in the Georgia portion of the SGR basin suggest there are porous zones in the J/T_R sandstones that could be used for geologic storage of CO_2 here. These porous zones will need to be far away from the transfer fault zones identified by Hefner (2013) to ensure containment of injected CO_2. It also needs to be stressed that the SGR basin covers area in four states (South Carolina, Georgia, Alabama and Florida). The injection simulations conducted in this study were limited to one small area. Consequently, there is enormous potential for CO_2 storage in other portions the basin and further research needs to be done to locate these suitable areas.

The suggested next step of the research are to:

1) Continue with the fault permeability analysis on a logarithmic scale approach. 0 mD, 1 mD and 100 mD are a good foundation for future fault leakage analyses adding 10 mD, 1000 mD and 10,0000 mD and use these results to create fault leakage coefficients and a permeability vs leakage graph one could use to estimate the leakage in their fault system.
2) Use available software such as the Computer Modelling Group Ltd. WinProp module to simulate the CO_2/basalt mineralization to calculate the mineralization rate as well the volume of mineral trapping after a 100 year simulation.

References

Akintunde, O.M., Knapp, C., and J.H. Knapp (2012), Petrophysical characterization of the South Georgia Rift Basin for supercritical CO_2 storage: a preliminary assessment. *Environmental Earth Science*, 70:2971-2985

Akintunde, O.M., Knapp, C., Knapp, J.H., and D.M. Heffner (2013), New constraints on buried Triassic basins and regional implication for subsurface CO_2 storage from the SeisData6 seismic profile across the Southeast Georgia coastal plain. *Environmental Geosciences*, Vol. 20. NO. 1, pp. 17-29

Bachu, S. (2000), Sequestration of CO2 in geological media in response to climate chang: road map for site selection using the transform of geological space into the CO2 phase space: *Energy Conversion and Management*, v. 43, p. 87-102.

Bachu, S., and B. Bennion (2008), Effects of in-situ conditions on relative permeability characteristics of CO2-brine systems: *Environmental Geology*, v. 54, p. 1707-1722.

Basburg, B., and F Gumrah (2005), Simulating the effects of deep saline aquifer properties on CO2 sequestration. 6th Canadian International Petroleum Conference, Calgary Canada.

Brantley, D.T., Shafer, J.M., and V. Lakshmi (2015), CO_2 Injection Simulation into the South Georgia Rift Basin for Geologic Storage: A Preliminary Assessment, *Environmental Geosciences* (in press).

Bacon, D.H., White, M.D., Gupta, N., Sminchak, J.R., and M.E. Kelley (2009), CO2 sequestration potential in the Rose Run Formation at the Mountaineer Power Plant, New Haven, West Virginia, in M. Grobe, J. C. Pashin, and R. L. Dodge, eds., Carbon dioxide sequestration in geological media—State of the science: AAPG Studies in Geology 59, p. 553–570.

Behtham, M., and G. Kirby (2005), CO2 Storage in Saline Aquifers: Oil & Gas and Technology - Rev. IFP, v. 60, no. 3, p. 559-567.

Boden, T.A., Kaiser, D.P., Sepanski, R.J., and F.W. Stoss (1994), Trends '93: A compendium of Data on Global Climate. Oak Ridge, Tennessee 37831: Oak Ridge National Laboratory - Sponsored by DOE - Environmental Sciences Division.

Boxiao, L., Tchelepi, H.A., and S.M. Benson (2012), The Influence of Capillary Pressure Entry-Pressure Representation on the Rate of CO2 solubility Trapping: Proceedings, TOUGH Symposium; September 17-19, 2012. Berkeley, California: Lawrence Berkeley National Laboratory, 1-8.

Canadell, J.G., Le Quere, C., and M.R. Raupach (2007), Contributions to accelerating atmospheric CO2 growth from economic activity, carbon intensity, and efficiency of natural sinks: *Proceedings of the National Academy of Sciences*, U.S.A, v. 104, no. 47, 18866-70.

Chowns, T.M., and C.T. Williams (1983), Pre-Cretaceous rocks beneath the Georgia Coastal Plain - regional implications, in G.S. Gohn, ed., Studies Related to the Charleston, South Carolina Earthquake of 1886-Tectonics and seismicity: U.S. Geologic Survey Professional Paper 1313, 42 p.

Cinar, Y., and A. Riaz (2014), Carbon dioxide sequestration in saline formations: Part 2-Review of multiphase flow modeling. *Journal of Petroleum Science and Engineering*, 124 pp. 381-398. doi:10.1016/j.petrol.2014.07.023

Clendenin, C.W., Waddell M.G., and A.D. Addison (2011), Reactivation and overprinting of the South Georgia Rift Extension. Geological Society of America Annual Meeting Oct. 9-11, Minneapolis MN. Abstra. Program 43 (5), p 551.

Clendenin, C.W. (2013), Insights into mode of the South Carolina rift extension in eastern Georgia, USA. *Tectonophysics*, 608, p 613-621.

Copsey, R. (2014) About C Tech: <www.ctech.com>. Accessed July 2014.

Damsleth, E. (1994), Mixed Reservoir Characterization Methods. Proceedings from the Centennial Petroleum Engineering Symposium, Tulsa, Oklahoma.

Daniels, D.L., Zietz, I., and P. Popenoe (1983), Distibution of subsurface lower Mesozoic rocks in the southeastern United States as interpreted from regional aeromagnetic and gravity maps, in Gohn, G.S., ed., Studies Related to the Charleston, South Carolina Earthquake of 1886-Tectonics and Seismicity: United States Geological Survey Professional Paper 1313, p. K1-K24.

Delshad, M., Wheeler, M.F., and X. Kong (2010), A Critical Assessment of CO2 Injection Strategies in Saline Aquifers. Society of Petroleum Engineers Western Regional Meeting, 27-29 May, Anaheim, California, USA. SPE-132442-MS.

Deng, H., Stauffer, P.H., Dai, Z., Jiao, Z, and R.C. Surdam (2012), Simulation of industrial-scale CO_2 storage: multi-scale heterogeneity and its impacts on storage capacity, injectivity and leakage. *International Journal of Greenhouse Gas Control*, 10, 397–418

Doyen, P.M. (2007), Seismic Reservoir Characterization: An Earth Modelling Perspective: Houten, The Netherlands, European Association of Geoscientist and Engineers, 255 p.

Duan, Z., and R. Sun (2003), An improved model calculating CO_2 solubility in pure water and aqueous NaCl solutions from 273 to 533 K and from 0 to 2000 bar. *Chemical Geology*, 193, 257–71

Duan, Z., Sun, R., Zhu, C., and I-M. Zhou (2006), An improved model for the calculation of CO_2 solubility in aqueous solution containing Na+, K+, Ca2+, Mg2+, Cl _ , and SO4 2_. *Marine Chemistry*, 98, 131–9

Frangeul, J., Nghiem, L., and E. Caroli (2004), Sleipner/Utsira CO_2 geological storage: full field flow and geochemical coupling to assess the long term fate of the CO_2. Proceedings AAPG Annual Conference, Paper AAPG 86278.

Ghomian, Y., Pope, G.A., and K. Sepehrnoori (2008), Reservoir Simulation of CO_2 Sequestration Pilot in Frio Brine Formation, USA Gulf Coast: Energy, v. 33, p. 1055-1067.

Goldberg, D.S., Takahash,i T., and A.L. Slagle (2008), Carbon dioxide sequestration in deep-see basalt. *Proceedings of the National Academy of Sciences of the United States of America*, Vol 105 No 29 pp. 9920-9925. doi: 10.1073pnas.0804397105

Heffner, D.M., Knapp, J.H., Akintunde, O.M., and C.C. Knapp (2011), Preserved extent of Jurassic flood basalt in the South Georgia Rift: A new interpretation of the J horizon. *Geology,* Vol. 40 Issue 2, pp. 167

Hefner, D.M. (2013), Tectonics of the South Georgia Rift, Doctoral dissertation, University of South Carolina, Columbia, SC, 178 p.

Hollon, B., Mainali, P., Dix, M., Fu, R., Houghton, N., and M. Waddell (2014), Whole Rock Bulk Geochemistry in Evaluating a CO_2 Injection Well. Proceedings from the AAPG Annual Convention and Exhibit 2014, Houston, TX

Houghton, J. (1997), Global Warming: The Complete Briefing, 2nd ed.: Cambridge University Press, 267 p.

Hou, Z.M., Gou, Y., Taron, J., Gorke, U.J., and O. Kolditz (2012), Thermo-hydro-mechanical modeling of carbon dioxide injection for enhanced gas-recovery (CO2-EGR): a benchmarking study for code comparison. *Environmental Earth Science* 67 (2) pp. 549-561. DOI 10.1007/s12665-012-1703-2

Keeling, C.D., and T.P. Whorf (2004), Atmospheric CO2 from Continious Air Samples At Mauna Loa Observatory, Hawaee, U.S.A.: Oak Ridge, Tenn. U.S.A., Carbon Dioxide Information Center, Oak Ridge National Laboratory.

Kempka, T., and M. Kuhn (2013), Numerical Simulations of CO_2 arrival times and reservoir pressure coincide with observations from the Ketzin pilot site, Germany. *Environmental Earth Science* 70(8) pp. 3675-3685

Klitgord, K.D., Popenoe, P., and H. Schouten (1984), Florida: A Jurrasic transform plate boundary: *Journal of Geophysical Research*, v. 89, p. 7753-7772.

Leung, D.C.Y., Caramanna, G., and M.M. Maroto-Valer (2014), An overview of current status of carbon dioxide capture and storage technologies. *Renewable and Sustainable Energy Reviews*. 39 pp. 426-443. doi:10.1016/j.rser.2014.07.093

Mammoli, A.A., and C.A. Brebbia (2011), *Computational Methods in Multiphase Flow VI.* WIT Transactions on Engineering Sciences, Vol. 70, WIT Press. South Hampton, United Kingdom. p 312

McBride, J.H. (1991), Constraints on the structure and tectonic development of the Early Mesozoic South Georgia Rift, southeastern United States; Seismic Reflection Data Processing and Interpretation: *Tectonics*, v. 10, no. 5, p. 1065-1083.

Mercer, J.W., and R.R. Faust (1981), *Ground-Water Modeling*. National Water Well Association, Dublin, Ohio. 60 pp.

Micheal, K., Golab, A., Shulakova, V., Ennis-King, J., Allinson, G., Sharma, S., and T. Aiken (2010), Geological Storage of CO2 in saline aquifers - A review of the experience from exiting storage operations*: International Journal of Greenhouse Gas Control*, v. 4, p. 659-667.

Mohammed, A., Ekoja, G.A., Adeniyi, A.A., and A.B. Hassan (2012), Modelling Long Term CO2 in Saline Aquifers: *International Journal of Applied Science and Technology*, v. 2, no. 10, p. 53-62.

Mukhopadhyay, S., Doughty, C., Bacon, D., Bacci, G., Govindan, R., Shi, J., Gasda, S., Ramanathan, Nicot, J-P., Hosseini, S., and J.T. Birkholzer (2012), Preliminary Model-Comparison Results from the SIM-SEQ Project using TOUGH2, STOMP, ECLIPSE, and VESA Approach. Proceedings from the TOUGH Symposium. Lawrence Berkeley National Laboratory, Berkeley, CA. Sept 17-19, 2012.

Nasvi, M.C.M., Ranjith, P.G., Sanjayan, J., and A. Hague (2013), Sub- and super-critical carbon dioxide permeability of wellbore materials under geological

sequestration conditions: An experimental study. *Energy* 54 pp. 231-239. http://dx.doi.org/10.1016/j.energy.2013.01.049
Neftel, A., Friedli, H., Moor, E., Lotscher, H., Oeschger, H., Siegenthaler, U., and B. Stauffer (1994), Historical CO2 record from the Siple Station ice core, In Trends: A Compendium of Data on Climate Change: Oak Ridge, Tenn. U.S.A., Oak Ridge National Laboratory, U.S. Department of Energy - Carbon Dioxide Information Analysis Center.

Nelson, P.H., and J.E. Kibler (2003), A Catalog of Porosity and Permeability from Core Plugs in Siliciclastic Rocks, U.S.G.S. open file report 03-420: Denver, CO, Department of the Interior.

Olsen, P.E. (1997), Stratigraphic record fo the early Mesozoic breakup of Pangea in the Laurasia-Gondwana rift system: Annual Review of Earth and Planetary Sciences, v. 25, p. 337-401.

Omambia, A.N., and Y. Li (2010), Numeric modeling of carbon dioxide sequestration in deep saline aquifers in Wangchang Oilfield-Jianghan Basin, China: *Journal of American Science*, v. 6, p. 178-187.

Park, Y., Kim, D.Y., Lee, J.W., Huh, D.G., Park, K.P., Lee, J., and H. Lee (2006), Sequestering carbon dioxide into complex structures of naturally occurring gas hydrates. *Proceedings of the National Academy of Sciences of the United States of America*. Vol. 103 No 34 pp. 12690-12694. doi: 10.1073 pnas.0602251103

Pires, J.C.M., Martins, F.G., Alvim-Ferraz, M.C.M., and M. Simoes (2011), Recent developments on carbon capture and storage: An overview. *Chemical Engineering Research and Design*. Vol 89 pp. 1446-1460. doi:10.1016/j.cherd.2011.01.028

Pruess, K. (2005), ECO2: A TOUGH2 Fluid Property Module for Mixtures of Water, NaCl, and CO2: University of California, Berkeley, CA 64720, Lawrence Berkeley National Laboratory - Earth Sciences Division.

Pruess, K., and N. Spycher (2006), ECO2N - A New TOUGH2 Fluid Property Module for Studies of CO2 Storage in Saline Aquifers: University of California, Berkeley, CA 64720, Lawrence Berkeley National Laboratory - Earth Sciences Division.

Remy, N., Journel, A.G., Boucher, A., and J. Wu (2007), Stanford Geostatistics Modeling Software: First Edition. Stanford University, Stanford, California.
Riaz A, Cinar Y (2014) Carbon dioxide sequestration in saline formations: Part 1-Review of the modeling of solubility trapping. Journal of Petroleum Science and Engineering. 124 pp. 367-380. http://dx.doi.org/10.1016/j.petrol.2014.07.024

Rine, J.M., Hollon, B., Fu, R., Houghton, N., and M. Waddell (2014), Diagenetic and Burial History of a Portion of the Late Triassic South Georgia Rift Basin Based

on Petrologic and Isotopic (o18) Analyses of Sandstones from Test Borehole Rizer #1, Colleton County, SC. Proceedings from the AAPG Annual Convention and Exhibit 2014, Houston, TX

Rutqvist, J., Birkholzer, J., Cappa, F., and C.F. Tsang (2007), Estimating maximum sustainable injection pressure during geological sequestration of CO_2 using coupled fluid flow and geomechanical fault-slip analysis. *Energy Conversion and Management*. 48, 1798–807

Ryan, M.P., Stuphin, D.M., Daniels, D.L., Pierce, H.A., and J.P. Smoot (2002), Three Dimensional Compartmentalization on Subsurface Ground Water Flow in Eastern North American Mesozoic Basins: American Geophysical Union, Spring Meeting: Washington, DC, AGU, Abstract # H22C-09.

Sasaki, K., Fujii, T., Niibori, Y., Ito, T., and T. Hashida (2008), Numerical simulation of supercritical CO2 injection into subsurface rock masses: *Energy Conversion & Management*, v. 49, p. 54-61.

Schlische, R.W., Withjack, M.O., and P.E. Olsen (2003), Relative timing of CAMP rifting continental breakup and basin inversion: tectonic significance, in W.E. Hames, J.G. McHone, P.R. Renne, and C. Ruppel, eds.,The Central Atlantic Magmatic Province: Insights from fragments of Pangea: *American Geophysical Union, Geophysical Monograph Series*, v. 136, p. 33-59.

Saadatpoor, E., Bryant, S.L., and K. Sepehrnoori (2009), New Trapping Mechanism in Carbon Sequestration. *Transport in Porous Media.* Vol 83, Issue 1, pp. 3-17. DOI 10.1007/s11242-009-9446-6

Schlumberger (2015) Petrel™ E&P Software Platform. http://www.software.slb.com/products/platform/Pages/petrel.aspx. Accessed November 2014

Shafer, J.M., and D.T. Brantley (2011), Characterizing a Geologic Formation: *Chemical Engineering Progress,* p. 50-52.

Shu, L., Ruina, X., and J. Peixue (2012), Effect of reactive surface area of minerals on mineralization trapping of CO2 in saline aquifers. Petroleum Science Vol 9 Issue 3 pp. 400-407. DOI 10.1007/s12182-012-0224-7

Solomon, S., Plattner, G.K., Knutti, R., and P. Friedlingstein (2009), Irreversible climate change due to carbon dioxide emissions: *Proceedings of the National Academy of Science* U.S.A, v. 106, no. 6, p. 1704-9.

Thibeau, S., and L. Nghiem (2007), A modeling study of the role of selected minerrals in enhancing CO2 mineralization during CO2 aquifer storage. SPE

Annual Technical Conference and Exhibition, Anaheim, USA. http://dx.doi.org/10.2118/109739-MS

United States Department of Energy (2006) Carbon Sequestration Atlas of the United States and Canada. Pittsburg, PA, National Energy and Technology Laboratory.

United States Department of Energy (2008) Carbon Sequestration Atlas of the United States and Canada. Pittsburg, PA, National Energy and Technology Laboratory.

Vargaftik, N.B. (1975), *Tables on the Thermophysical Properties of Liquids and Gases*, 2nd Ed: New York, John Wiley & Sons.

Vleit, J. van, White, R., and S. Dragicevic (2009), Modeling urban growth using a variable grid cellular automaton: Computer, *Environment and Urban Systems*, v. 33, no. 1, p. 35-43.

Waddell, M.G., Addison, A.D., Brantley, D., and C. Knapp (2011), Reservoir and caprock assessment using existing seismic and well data for CO_2 geologic sequestration in the South Georgia Rift basins of the lower Coastal Plain of SC. AAPG Annual Conference and Exhibition. Abstra. 90124

Waddell, M.G., Brantley, D., and A.D. Addison (2014), Characterization of the South Georgia Rift Basin for Source Proximal CO_2 Storage; Final Technical Report. South Carolina Research Foundation, 1600 Hampton Street, Columbia, SC 29208

Withjack, M.O., Schlische, R.W., and P.E. Olsen (1998), Daichronous Rifting, Drifting, and Inversion on the Passive Margin of Central Easter North America: An Analog for Other Passive Margins: *The American Association of Petroleum Geologist Bulletin*, v. 82, p. 817-835.

Yamamoto, H., Zhang, K., Karasaki, K., Marui, A., Uehara, H., and N. Nishikawa (2009), Numerical investigation concerning the impact of CO2 geologic storage on regional groundwater flow: *International Journal of Greenhouse Gas Control*, v. 3, p. 586-599.

Zang, K., Moridis, G., and K. Pruess (2011), TOUGH+CO2: A multiphase fluid-flow simulation for CO2 geologic storage sequestration in saline aquifers. *Computers and Geosciences.* Vol 37 Issue 6 pp. 714-723. DOI: 10.1016/j.cageo.2010.09.011

Zhuo, Q,. JBirkholzer, J.T., Rutqvist, J., and C.F. Tsang (2007), Sensitivity Study of CO2 Storage Capacity in Brine Aquifers with Closed Boundaries: Dependence on Hydrogeological Properties: Sixth Annual Conference on Carbon Capture and

Sequestration; University of California, Berkeley, Berkeley CA 64720, DOE-NETL Earth Sciences Division, Lawrence Berkeley National Laboratory.

Zoback, M.D., and S.M. Gorelick (2012), Earthquake triggering and large-scale geologic storage of carbon dioxide. *Proceeding of the National Academy of Sciences of the United States of America*. Vol 109 No 26 pp.10164-10168. doi/10.1073/pnas.1202473109